https://doi.org/10.1595/205651323X16778518231554 *Johnson Matthey Technol. Rev.*, 2023, **67**, (4), 371–401

JOHNSON MATTHEY
TECHNOLOGY REVIEW

technology.matthey.com

Microbubble Intensification of Bioprocessing

The role of direct microorganism and bubble interactions

P. D. Desai
Perlemax Ltd, 318 Broad Lane, Kroto Innovation Centre, Sheffield, S3 7HQ, UK

W. B. Zimmerman*
Department of Chemical and Biological Engineering, Mappin Street, University of Sheffield, Sheffield, S1 3JD, UK

***Email:** w.zimmerman@sheffield.ac.uk

PEER REVIEWED

Received 1st December 2022; Revised 16th February 2023; Accepted 3rd March 2023; Online 3rd March 2023

Microbubbles are famed for their large surface area-to-volume ratio, with the promise of intensification of interfacial phenomena, highlighted by more rapid gas exchange. However, for bioprocessing, it has been recognised for many decades that surfactant-rich fermentation media hinders mass transfer and possibly other interfacial processes due to surfactant loading on the interface. This article focuses on the roles of microbubble size and bubble bank, dispersed microbubbles that are sufficiently small to be non-buoyant, in mediating other modes of interfacial transfer *via* collisions with microorganisms and self-assembled clusters of microorganisms and microbubbles. These provide a more direct route of mass transfer for product gases that can be released directly to the microbubble with ~10^4 faster diffusion rates than liquid mediated gas exchange. Furthermore, secreted external metabolites with amphoteric character are absorbed along the microbubble interface, providing a faster route for liquid solute transport than diffusion through the boundary layer. These mechanisms can be exploited by the emerging fields of symbiotic or microbiome engineering to design self-assembled artificial lichen dispersed structures that can serve as a scaffold for the selected constituents. Additionally, such designed scaffolds can be tuned, along with the controllable parameters of microbubble mediated flotation separations or hot microbubble stripping for simultaneous or *in situ* product removal. Staging the product removal thus has benefits of decreasing the inhibitory effect of secreted external metabolites on the microorganism that produced them. Evidence supporting these hypotheses are produced from reviewing the literature. In particular, recent work in co-cultures of yeast and microalgae in the presence of a dispersed bubble bank, as well as anaerobic digestion (AD) intensification with dispersed, seeded microbubbles, is presented to support these proposed artificial lichen clusters.

1. Introduction

This paper should be read as a continuation of the review by Gilmour and Zimmerman (1) of now 14 years of exploitation of fluidic oscillation (FO) generated microbubbles (1–999 μm). This approach, as the counterpart to high energy efficiency of the generation, maintains laminar flow with a low shear environment, that is not otherwise found with microbubble generation mechanisms. Generally, high energy dissipation is required for the generation of microbubbles by other methods, which can lyse cells due to the highly turbulence shear induced. The focus of this paper is about the collisions between microbubbles and microorganisms that have been exploited traditionally for flotation and absorptive bubble separation bioprocesses, but due to the laminar

character of the flow field, can be controlled and even designed for either distinct fermentation and separation bioprocesses, or simultaneous and even *in situ* product removal.

Mass transfer in bioprocessing has a canonical description for the microorganism uptake of dissolved gases subsequent to the dissolution of the gas from a bubble phase, controlled by the boundary layer dynamics of the bubble. The opposite mechanism to this dosing scenario is the stripping of secreted gases from the microorganism through the liquid medium to the microbubble. The received wisdom is that microbubbles, with much greater interfacial area for the volume of bubble phase injected, simply accelerate this canonical liquid mediated mass transfer process. The two-film theory for gas-liquid mass transfer posits that the mass transfer flux is proportional to the surface area of the gas-liquid interface, so *prima facie* this canonical mechanism should be accelerated by microbubble throughput. The theory (2) describes a seven-stage mechanism for mass flux that is limited by the two-film transfer as the slowest step.

But is the canonical bubble-throughput and liquid mediated mass transfer mechanism the only mass transfer mechanism occurring in fermentation processes? Are other mechanisms potentially as important or even dominant when the bubble phase diameter decreases? We pose that there are three more mechanisms that are also important in the microbubble regime.

The second mechanism that is classically well understood is microbubble-microorganism collisions. It is clear that with a constant volumetric flow rate of bubble phase, decreasing the bubble size increases dramatically the microbubble number density. Flotation separations rely on successful collisions between microbubbles and particles to form flocs, with the overall buoyancy of the floc less than the surrounding liquid media, so that it rises, collects at the top of the liquid media, and is skimmed off. The success of the collisions depends on the sticking factor of the collision, which is determined by the electronic attractiveness (repulsion) of the particle and bubble. The overall rate of separation depends on this sticking factor and the rate of bubble-particle collisions. Hydrodynamic collision theory shows that the rate of collisions depends crucially on the particle-bubble aspect ratio: particles and bubbles of similar sizes have a much higher collision cross-section than when either is substantially larger or smaller than the other. The collision rate drops off when this ratio deviates from unity, and dramatically when it is less than 0.1 or more than 10.

If a collision is unsuccessful, i.e. does not result in a floc forming, it still has the effect of exposing the membrane or cell wall of the microorganism to the gas phase of the microbubble, and *vice versa*. If the microorganism secretes gases, its membrane or cell wall is suffused with the gas, so it has a direct contact with the extracting microbubble for rapid exchange. The diffusion of a gas within a gas phase is approximately 10^4 faster than through a liquid. The dosing mechanism is also faster by this factor, locally. With the collision rate dramatically faster for microbubbles that are similar in size to the microorganism, this mechanism is not proportional to the interfacial area of the bubble phase, but highly selective for microbubble size. Classically, coarse (>4 mm diameter) and fine bubbles (1–4 mm diameter) are so much larger than the microorganisms in fermentation that this mechanism is immaterial. The collision cross-section in the classical case is negligibly small.

The other two mechanisms explored here are based on microbubble phase accumulation. Coarse and fine bubbles have a significantly strong buoyant force that their dynamics are predictable along the profile from injection, rise, dispersal along the top liquid surface with the headspace gas, possibly the build-up of foam, and eventual bursting of the bubbles which releases their contents to the headspace. The profile is sufficiently predictable that the throughput of bubbles has injection rate nearly equal to off gas production rate, which is manifestly a (pseudo) steady state, there is negligible accumulation of bubbles in the liquid phase, while the dissolution of gas is balanced by the mass transfer, as measured by dissolved oxygen (DO) probes, for instance. Mass balance is satisfied for the conservation of the gas *via* the canonical mechanism.

With microbubbles, the buoyant forces are dramatically weaker. For, say, 20 μm diameter microbubbles, the rise time for a meter is more than a day. Any liquid currents, even those induced by the injection of the bubble phase themselves, is likely to entrain 100 μm diameter microbubbles so that they are suspended and circulating in the liquid phase. Transient simulations of microbubble injections show that the phase fraction of microbubbles suspended and circulating increases over time, but eventually plateaus as a steady level reflecting a much longer residence time (3).

This phenomenon has been called a ‘bubble bank’ (4) due to its effect as an additional storage capacity for dissolved gases. Transient studies of dissolution show the achievement of saturation with,

say, DO probes. The rate of degassing, however, is noticeably slower if there is a bubble bank. The biological uptake of DO, for instance, can achieve increased biomass growth at saturated levels of DO after sparging has ceased. This accumulation effect could still be liquid mediated mass transfer, but not a steady state phenomenon.

The other potential accumulation of microbubbles is the successful collision of microbubbles with biomass, i.e. floc formation that does not create sufficient buoyancy difference to float or sediment the floc. The flocs maintain suspension, permitting direct microbubble to microorganism gas exchange within the floc. Since microorganisms can secrete substantial amounts of extracellular metabolites as well as comprising amphoteric molecules within the membranes or cell walls, similar size microbubbles and biomass particles could populate the interface of 'captured' microbubble with surfactant materials, effectively blocking the gas transfer from bubble to the surrounding liquid media. This mechanism was once credited for the futility of using microbubbles, as surfactant blockage of the interface would interrupt gas exchange *via* the canonical liquid mediated mechanism. It is, however, a strong supporting argument for direct microbubble to microorganism gas exchange in the case that microbubbles are successfully captured.

The last of these four competing mechanisms for microbubble mediated gas exchange gives rise to the conjecture that gas exchange can be intensified in co-cultures or consortium of microorganisms. Microorganisms are known to be motile. Tropism and taxis are essential drives in the viability of microorganisms. If a microbubble provides a nutrient source to one species present in a consortium *via* direct contact, the exchange of a product gas to the microbubble makes it a nutrient source for a species that uptakes that gas. The tropism or taxis drive then coordinates the second species, with the secreted metabolite and embedded surfactant effects providing stability to the microbubble-microorganism assembly. It is well known, for instance, that microbubbles utilised for medical imaging and drug delivery are stabilised by surfactants, avoiding gas-liquid exchange. The local ecology of microbubble complexed microorganisms is dramatically accelerated by the gas phase of the microbubble being the exchange media over the bulk liquid media. This mechanism was introduced originally by Gilmour and Zimmerman (1) as Desai artificial lichen (DAL), subsequently also termed Desai microbubble scaffolds (DMS). One of the first conjectured scaffolds was the seeding of a bubble bank in anaerobic fermentation of yeast to produce ethanol, reported by Gilmour and Zimmerman (1) to have increased the production rate of ethanol, through more rapid off gas evolution and lower liquid content, by 120% over the control of no bubble bank injection. Raghavendran *et al.* (5) reported that this system expressed a substantially different level of proteins, mostly associated with cell wall maintenance and regulation, than perfusion bioreactors during the aerated, propagation phase, with the same levels of DO maintained.

The purpose of this review article is to explore microbubble mediated intensification of bioprocessing, viewed through the prism of the competing mechanisms for gas exchange in the exposition here. Some accelerations of metabolic production rates observed with microbubble deployment are simply inexplicable by the canonical liquid mediated theory, due to the nutrient or product gases being practically insoluble in water, for instance. Section 2 reviews mass transfer theory and microbubble mediated mass transfer, with the update on Gilmour and Zimmerman provided by hot microbubble stripping for ammonia-water separations (6) demonstrating exploitation of rapid internal mixing and differential vaporisation rates at microbubble interfaces, even in heavily surfactant-laden wastewater media, including centrate of anaerobic digesters. Section 3 reviews absorptive (micro)bubble separations aiming at applications for bioprocessing. Section 4 reviews the evidence and supporting arguments for microbubble mediation, by direct bubble and microorganism interactions, for symbiotic and microbiome engineering, where DAL or DMS clusters can be designed for fermentation and separation, with several different routes for optimality. Section 5 summarises the exposition and draws conclusions.

2. Microbubble Mediated Gas Transfer in Biocultures

Microbubbles are usually touted for the obvious feature that mass transfer across the gas-liquid interface should be faster than the same volume of gas distributed in conventional fine bubbles (1–4 mm in diameter). However, this was not the received wisdom historically. To understand the historical opposition to intensification of mass transfer by microbubbles in bioreactors, the canonical conceptual model for mass transfer must first be described. It comes from the classic textbook of Bailey and Ollis (2). They modelled gas

exchange between a bubble and liquid dispersed microorganism from seven resistances, expressed with the mass transfer driver between the nutrient gas rich bubble and the nutrient gas starved microorganism:

a) Diffusion from bulk gas to the gas-liquid interface
b) Transfer of the gas through the gas-liquid interface
c) Diffusion of the gas through the liquid boundary layer surrounding the bubble interface to the bulk liquid
d) Transport of the gas through the bulk liquid to the boundary layer surrounding the microorganism
e) Diffusion of the gas through the boundary layer to exterior boundary of the region of the community of microorganisms
f) Diffusion through the community to the envelope of the microorganism
g) Active or passive transport through the envelope and to the intracellular site of metabolism.

Bailey and Ollis (2) then analyse this scenario to conclude that the mass transfer flux, J, is described, at a pseudo-steady state identical across all seven intermediate mechanisms above, to Equation (i):

$$J = K_L a(c_l^* - c_l)V \quad \text{(i)}$$

where, Equation (ii):

$$\frac{1}{K_L} = \frac{1}{k_l} + \frac{1}{Hk_g} \quad \text{(ii)}$$

are the resistances in series for the overall resistance of the presumed limiting (slowest) mass transfer step, the gas traversing the gas-side, interfacial equilibrium and then the liquid side boundary layers of the bubble. This is often called the two-film transport problem. k_l, k_g are the film mass transfer coefficients for liquid and gas, respectively; H is the Henry's law coefficient for liquid solubility; K_L is the overall mass transfer coefficient; c_l is the liquid concentration of the dissolved gas; c_l^* is the concentration of the dissolved gas in the liquid in equilibrium with the gas phase concentration; a is the surface area of the entire bubble phase divided by the volume of the bubble phase, also termed the specific surface area.

Bailey and Ollis (2) presented this paradigm in the context of oxygen transfer for aerobic microorganisms, for which in the applications of the day, the assumption was that the microorganisms were oxygen starved and therefore mass transfer was the limiting rate for the metabolism. With hindsight, this model does not describe microbubble gas transport processes for soluble gases like O_2 and CO_2 particularly accurately, from the perspective of Equation (iii):

$$a_{microbubble} = 10^{1-3}\, a_{fine\ bubble} = 10^{2-4}\, a_{coarse\ bubble} \quad \text{(iii)}$$

Zimmerman *et al.* (7) showed that with microalgal growth in a 2 m^3 pilot plant bioreactor fed by ~1 m^2 of microporous diffusers with FO microbubbles of combustion exhaust gas, the off-gas was in equilibrium with the exhaust gas feed, having stripped the O_2 levels to equilibrium and the CO_2 dosed was at saturation. The only correlation in the daily growth rates was with average daily solar intensity. The system was not mass transfer limited, but rather metabolic limited. Similarly, with aerated yeast propagation, Hanotu *et al.* (8) were able to demonstrate pseudosteady-state operation at any level of DO concentration between zero and saturation, by variation of the microbubble superficial gas flowrate. In the prior literature, DO concentration crashes to zero very quickly as the yeast were oxygen starved. This study showed that mass transfer rate could be matched to oxygen uptake rate (OUR) so that any level of DO concentration can be stable, i.e. mass transfer rate could exceed OUR and therefore be tuned to achieve a steady DO level.

These two scenarios of 'overdosing' and tuned dosing are both outside the assumptions underpinning Equation (i), some other flux than the bubble films is rate limiting. It is now routinely the case with laboratory bench bioreactors from common suppliers, such as Infors AG (Switzerland) and Pall Life Sciences (now Cytiva, USA), that perfusion recirculation achieves saturated dissolved gas concentrations of soluble gases, without recourse to microbubbles. However, laboratory bench bioreactors can use high mechanical power intensities to achieve sufficient mixing for mass transfer to have high rates whilst concomitantly suffering from issues related to overheating within a system due to higher temperatures achieved by high metabolic rates. Scaling to industrial scale always results in imperfect mixing with slow mass transfer with impeller driven mixed vessels (9). Hence, energy efficient, low power consumption, FO generated microbubbles have an important role in large scale operations, since they achieve high liquid mixing efficiencies (3).

The historic opposition to microbubble implementation for mass transfer in fermenters, however, comes from two different veins of thought.

Firstly, the classic textbook of Clift *et al.* (10) reviewed the bubble dynamics and mass transfer characteristics for a range of different system properties. They assessed the influence of surfactants, particularly with bubbles in the surface tension dominated regime. They found a large variation in empirical relations for volumetric mass transfer coefficients, K_La, for intermediate-sized bubbles, which they explained by the different bubble generation techniques, measurement systems and system purities. Surfactant contamination was found to have a significant effect on smaller bubbles. In essence, decreasing bubble size introduced into fermenters would block mass transfer Step 2 in Bailey and Ollis' (2) resistance mechanisms by the surfactant occupancy of the microbubble interface. Fermentation media, particularly after significant residence time, abounds in surfactants. This objection may well be true. It is supported by Schulze and Schlunder (11) who noted the transition in mass transfer rates with smaller bubble size, as well as Rosso and Stenstrom (12) who observed 30–70% reduction in K_La with reduced bubble sizes in surfactant-rich media. Yet how can we then explain the panoply of studies reviewed by Gilmour and Zimmerman (1) where microbubbles injected into bioreactors have resulted in greater growth rates and metabolism?

A second objection to utilisation of microbubbles in fermenters is championed by Nienow (13), who showed that all conventional microbubble generation methods used in bioreactors lysed cells so were wholly ineffective. Since fluidic oscillator generated microbubbles were patented with priority date in 2008, they were out of scope for Nienow (13). Nienow argued cogently that the major cause of cell lysis by microbubble action is due to their bursting energetically at the gas-liquid surface separating the fermentation broth from the headspace. What separates FO generated microbubbles from those generated by earlier methods is laminar (FO) *vs*. turbulent flow. Hanotu *et al.* (14) estimated from exit velocities of microbubbles from microporous diffusers and air supersaturated liquid from nozzles in dissolved air flotation (DAF) that the energy dissipation is ~1000 fold lower with fluidic oscillation-generated microbubbles. Hence currents in conventional microbubble distribution systems result in short residence times relative to FO-generated microbubbles. As such, FO microbubbles must surely be saturated with water vapour, thus having much lower interfacial tension, so that bursting at the top gas-liquid surface of the fermenter has much lower stress. However, the conventional methods of microbubble generation have much greater shear stress imposed on microorganisms. These arguments, along with the observation of Zimmerman *et al.* (15) that there was no dead microalgae sediment in the bottom of the 2 m^3 pilot plant, lend credence to the lack of cell lysis with FO microbubbles. Since then, FO microbubbles have been implemented in several fermentation type and algal reactor systems demonstrating increased viability as opposed to lysis. Work carried out by Desai and Zimmerman (16), funded by PhycoNet, produced algae in a microbubble reactor and subsequently floated them with >99% viability achieved.

2.1 Paradigm Theory for Bubble Mediated Gas Transfer in Fermenters

The textbook of Bailey and Ollis (2) has nearly 10,000 citations on Google Scholar™ at the time of writing, with 25% using the words 'mass transfer' and 27% 'oxygen transfer'. So the header for this subsection must seem heretical. There are no competing theories in the literature for how gas transfer happens between cells or microorganisms and microbubbles. The canonical theory, as depicted in **Figure 1(a)** is that microbubbles transfer dissolved gas to or from the liquid media (dosing or stripping) and microorganisms or suspended cells exchange dissolved gas with the liquid media. The slowest step is the gas exchange due to the two boundary layer films internal and external to the bubble interface. This theory leads to a semi-empirical model of mass transfer (Equation (i)) that seemingly describes all bubble mediated mass transfer in the literature prior to FO microbubbles and perfusion-type laboratory bench bioreactors, where it is now exhibited that dosing rates can exceed metabolism which is no longer mass transfer limited.

The seeming universality of the mass transfer model, Equation (i), however, is no mathematical mystery. Mass transfer coefficients are estimated in only two ways for bubbles used for fermentation: (a) physical chemical, typically in media with no microorganisms or cells; (b) biological, in media with microorganisms or cells with active metabolism. The physical chemistry approach monitors dissolved gas, typically DO due to fast response probes, in a transient study from low DO levels (~20% of saturation) to high DO levels (~80%), with or without microbial action. The solution to the first order, ordinary

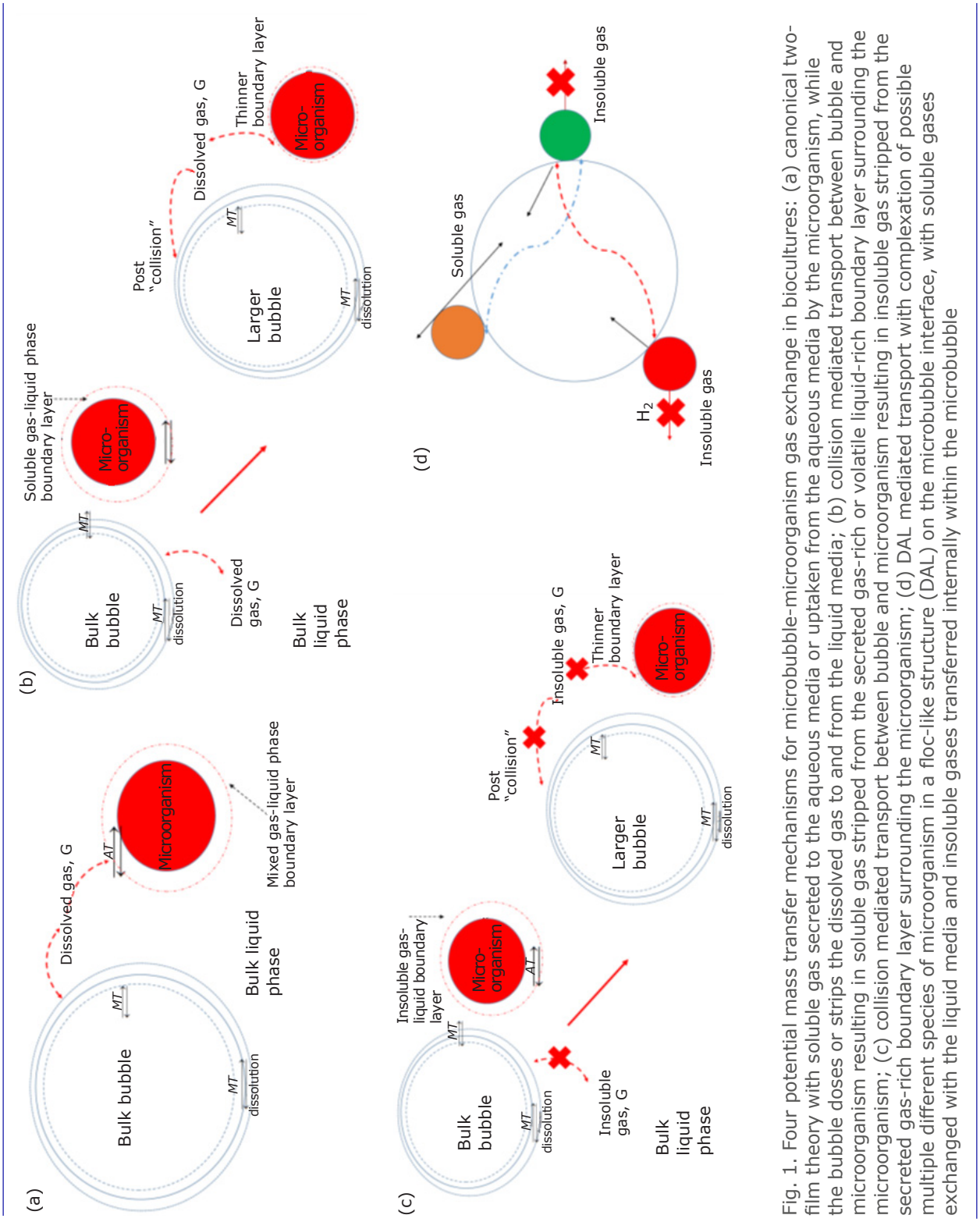

Fig. 1. Four potential mass transfer mechanisms for microbubble-microorganism gas exchange in biocultures: (a) canonical two-film theory with soluble gas secreted to the aqueous media or uptaken from the aqueous media by the microorganism, while the bubble doses or strips the dissolved gas to and from the liquid media; (b) collision mediated transport between bubble and microorganism resulting in soluble gas stripped from the secreted gas-rich or volatile liquid-rich boundary layer surrounding the microorganism; (c) collision mediated transport between bubble and microorganism resulting in insoluble gas stripped from the secreted gas-rich boundary layer surrounding the microorganism; (d) DAL mediated transport with complexation of possible multiple different species of microorganism in a floc-like structure (DAL) on the microbubble interface, with soluble gases exchanged with the liquid media and insoluble gases transferred internally within the microbubble

differential equation for accumulation of DO, Equation (i), is fitted to the DO transient data, to estimate K_La (17). The same approach conducted in activated sludge municipal wastewater results in a fitting parameter called αK_La, where the α-factor quantifies the reduction of mass transfer due to microbial action, for instance the 30–70% reduction observed by Rosso and Stenstrom (12). The high rates of superficial gas flow and the short time scale for aeration in these cases relative to metabolism permits the assumption that the αK_La estimate is about mass transfer alone, rather than combined microbial metabolic flux and mass transfer action.

The biological estimation approach was introduced by Bandyopadhyay and Humphrey (18), which they called the dynamical method. It starts from the modification of Equation (vii) to admit metabolic oxygen uptake, Equation (iv):

$$\frac{dc_l}{dt} = K_La(c_l^* - c_l) - rX \qquad \text{(iv)}$$

where r is the specific OUR per unit mass of fermenting microorganisms; X is the mass concentration of fermenting microorganisms in the fermenter. Note that the accumulation rate of dissolved gas concentration is set equal to the total mass transfer flux in Equation (iv). The observation that there is a critical dissolved gas concentration, $c_{l,crit}$ for which the accumulation rate vanishes, Equation (v):

$$\left.\frac{dc_l}{dt}\right|_{c_l = c_{l,crit}} = 0 \qquad \text{(v)}$$

It follows that a two-stage process can estimate both rX and K_La from alternating degassing and microbubble dosing. At the degassing stage, with Equation (v), i.e. steady $c_l = c_{l,crit}$, stop bubbling. Dissolved gas concentration linearly reduces, allowing the slope to estimate rX. Equation (vi):

$$\frac{dc_l}{dt} = -rX \qquad \text{(vi)}$$

Note that this model neglects off gas release through the top surface of the bioreactor.

At the dosing stage, restart bubbling from a lower level than $c_l = c_{l,crit}$. Estimate K_La from fitting the analytic solution to Equation (iv).

So Equation (vii):

$$\frac{dC}{dt} = K_La(c' - C) \qquad \text{(vii)}$$

It should be noted that by defining $c_l = C - rXt$, the new intermediate variable C satisfies Equation (vii) with the role of Equation (viii):

$$c' = c_l^* - \frac{rX}{K_La} \qquad \text{(viii)}$$

replacing c_l^*. This is mathematically identical to the conventional approach for estimating K_La from the analytic solution to Equations (i) and (vii). This two-stage dynamical process is exhibited by Ying *et al.* (19) for the periodic dosing of CO_2 by FO microbubbles into a microalgal bioreactor. Those authors showed that optimal periodic dosing achieved identical biomass production rates of microalgae to continuous dosing at a critical concentration $c_{l,crit}$ having tuned the gas throughput for steady dissolved gas level, but with approximately one twentieth of the gas throughput achieved by periodic dosing. One possible explanation is that dissolved CO_2 affects pH, whereas allowing CO_2 levels to drop periodically decreases pH shock. Microalgae naturally increase pH in the medium in absence of CO_2 dosing, providing a pH buffer. Consequently, the metabolism is less inhibited by pH effects in the periodic dosing case.

So why is there no mathematical mystery to the form of Equation (i)? Every process in the Bailey and Ollis (2) paradigm, with the possible exception of Step 7 if it is active transport, is a first order rate process. What that means, is that the process can be expressed mathematically as Equation (ix):

$$j_i = K_i(C_{input,i} - C_{output,i}) \qquad \text{(ix)}$$

Where j_i is the flux due to process i; K_i is the phenomenological coefficient found semi-empirically; and $(C_{input,i} - C_{output,i})$ is the driving force for the process i. De Donder (20) introduced the concept of chemical affinity, later popularised by Prigogine (21), that shows all non-equilibrium processes can be phenomenologically modelled as fluxes proportional to the driving force. When linear, first order processes are concatenated 'in series', they follow the resistances in series model that is shown in Equation (x):

$$\frac{1}{K_{overall}} = \sum_{i\ processes} \frac{1}{k_i} \qquad \text{(x)}$$

One might think that Henry's law for equilibrium, as shown in Equation (ii), violates this assertion, but actually, Henry's law is a simplification of a Langmuir-like evaporative rate law (6) of the form

Equation (ix). Henry's law enforces equilibrium at the interface, which is a very good approximation for rising microbubbles, according to Abdulrazzaq *et al.* (22). It follows that if any of the processes in Bailey and Ollis's paradigm are rate limiting, Equation (i) will hold, because it is impossible from performance data to separate the individual 'resistances' in Equation (x). For barely soluble gases, the Henry coefficient is very large, so $K_L \approx k_L$.

2.2 Microbubble-Microorganism Collision Mediated Gas Exchange

The processes in Bailey and Ollis's paradigm are not the only possible mechanisms for which first order rate processes can be ascribed. Microbubbles and microorganisms could collide. In Section 3, we will review absorptive (micro)bubble separation processes for downstream bioprocessing, for which it is well known that collision cross-section (collection efficiency) is maximal when two generalised particles (bubble and microorganism) are the same size. For much larger bubbles than microorganisms, which is true for conventional fine (1–4 mm diameter) and coarse (~1 cm diameter) bubbles, the collision cross-section is effectively zero. Only when bubbles and particles are within one order of magnitude in size does the cross-section become appreciable. Hence at the time Bailey and Ollis proscribed their paradigm for mass transfer, direct bubble to or from microorganism gas exchange from collisions or near collisions of the two generalised particles was unlikely to be a major mechanism, let alone the dominant mechanism.

2.2.1 Soluble Gases

It is, conceptually, just a modest change to the paradigm, with Step 6, entry of dissolved gas into the milieu of the microorganisms, overridden by Step 0, say, with the microbubble approaching within the milieu of the microorganisms. All the other processes are similar. **Figure 1(b)** suggests how this process works differently from the canonical mechanism, but in parallel for soluble gases. The microbubble and microorganism approach closely enough that their individual boundary layers overlap. Perhaps they even have a collision (elastic or inelastic) followed by their separation. While the boundary layers overlap or even when they are in direct contact, they can exchange gases. As shown in the schematic, the direction of exchange is stripping, with the soluble gases that is secreted as an external metabolite uptaken by the microbubble. The soluble gases that are nutrient gases for the microorganism can be uptaken from either the liquid or from the direct contact between the two generalised particles.

The mathematical modelling of this scenario follows the generic treatment of a chemical affinity as discussed concerning Equation (ix) and Equation (x). Generally, collisions and near collisions of generalised particles are binary processes described as first order in the concentration of each species. Since, at any given time, the number density of microorganisms is fixed in the fermenter, but microbubbles of the appropriate size distribution can be varied dynamically, the first order dynamics in microbubble number density is controlling the process. Furthermore, the other processes in the Bailey and Ollis paradigm are still first order in the driving force (concentration difference). This doubly first order (microbubble number density of the appropriate size and driving concentration) results in Equations (i) and (vii) still describing, semi-empirically, the rate of mass transfer. It is impossible to tell the difference between the canonical liquid mediated gas exchange and the collision mediated gas exchange. Both mechanisms participate, but which is dominant cannot be discerned from overall performance data.

Consider the possibility that microbubble interfaces are significantly loaded with surfactants, as posited by Clift *et al.* (10), so that the α factor blockage is severe in a fermentation media. Such microbubbles could still be mediating direct bubble to microorganism gas exchange, influencing the metabolism through collisions so that the dominant mechanism for dissolved gas uptake is direct, with the liquid mediated gas exchange much slower. Could we actually discriminate between the mechanisms in this scenario? The prediction from this theory is that the dissolved gas concentration level could be lower than fine bubbles with sufficiently long residence times in the dosing regime because the driver for liquid mediated gas exchange is identical, so with sufficiently high residence times for fine bubbles, the overall gas transfer should be the same for the same volumetric throughput. The microbubble mediated direct gas exchange with the microorganism, as the dominant microbubble mediated mechanism, would not involve significant transfer from the bubble to the bulk liquid, where the dissolved gas concentration is measured, due to the α-factor

Fig. 2. Two Tesař-Zimmerman (23) fluidic oscillators (DN50s) feeding one of two sequencing batch reactors (SBR) on a municipal wastewater treatment works

blockage. However, due to the faster direct gas exchange mechanism, the metabolism of the microorganisms should be faster. Assessing this prediction requires some means to measure the performance rate of the microbial metabolism.

Observations from early industrial-scale trials for wastewater aeration with FO provide some insight into the influence of microbial cultures and biomass in fermentation media. **Figure 2** shows the scale of fluidic oscillators with DN50 connectors, weighing 80 kg, feeding one of two sequencing batch reactors where the media is activated sludge on a municipal wastewater treatment works. The control SBR was fed air from a bank of blowers ducted into the same header, hence the same pressure source to both SBRs, outfitted with industry standard membrane slit diffusers. Both SBRs were fed activated sludge from the same source tank. The trials were planned to conduct a control SBR (no change from normal operation) and an active principle with FO tuned to achieve substantial decrease in bubble size from the standard 1–4 mm diameter fine bubbles, to approximately 500 μm on average, in clear water tests, using K_La inference (17) and acoustic bubble spectroscopy (ABS) for bubble size distribution estimation (16).

In clear water trials conducted simultaneously in the two SBRs, DO time profiles permitted the inference of K_La using Equations (i) and (vii) and demonstrated a 40% increase in K_La for the SBR outfitted with FO. One of the major challenges, however, with continuous industrial wastewater treatment plants is the lack of real-time monitoring of performance, which would necessitate sensors for measurements of chemical oxygen demand (COD) and biological oxygen demand (BOD). Such instrumentation for online inference does not yet exist, so continuous plants are monitored by sampling and laboratory analysis. The proxy for performance used in wastewater aeration for control is DO concentration.

With continuous flow treatment systems, DO historically correlates with COD and BOD reduction performance. With microbubbles, however, DO only captures the Bailey and Ollis mechanism for dissolution (**Figure 1(a)**). It does not capture the competing mechanism of direct microbubble to microorganism transfer, such as by collision (**Figure 1(b)**). But if the direct transfer mechanism is important, the DO level and performance correlation should not hold. With SBRs, the operator halts the cycle when the level of DO rises dramatically from a fairly constant, low level. During the low DO level regime, the BOD drops due to microbial action. Once the BOD has reached scarcity levels, microbial metabolism is subdued, and DO levels build up. Of course, the rise rate should be consistent with the αK_La fitting parameter for Equations (i) and (vii).

Indeed, the analysis of exponential rise periods in the datasets associated with the SBR field trials in **Figure 2** showed a 40% rise improvement for the active principle of FOs, maintaining the same relative improvement as the clear water trials. The surprise was that DO levels throughout the low DO metabolically active interval were lower for FO than for the control of steady flow. Nevertheless, the overall performance, time for metabolism to reduce BOD levels to scarcity, heralded by the rapid rise in DO, was faster for FO. These results are consistent with both direct by collision and conventional liquid mediated gas exchange occurring simultaneously.

2.2.2 Nearly Insoluble Gases

For insoluble gases, direct contact gas exchange is depicted by **Figure 1(c)**. The significant difference between soluble and insoluble gases is that dosing insoluble gases is a rare class of fermentation. Gas fermentation now has the connotation of fermentation by microorganisms that includes a nearly insoluble gas, almost exclusively methane, carbon monoxide or hydrogen, as a nutrient gas. The common soluble gas for aerobic metabolism is the co-nutrient oxygen. According to Kaye and Laby (24), the solubility of hydrogen gas is 0.16 mg l^{-1} at saturation with 1 atm at 293 K. Methane has 2.3 mg l^{-1} solubility under the same conditions, which is low but around

half of oxygen's solubility. At 2.8 mg l^{-1}, carbon monoxide is more soluble but still significantly less so than oxygen, which is known to be constrained by surfactant loading on the interface of microbubbles by the alpha factor. For such nearly insoluble gases, the concentration difference between the solubility limit and the dissolved gas concentration that serves as the driving force for mass transfer is already very weak (Equation (i)). Many fermentations are conducted around 37°C, so solubility drops even faster.

Worden *et al.* (25) pose a number of challenges for gas fermentation with synthesis gas (CO + H_2), posing the low gas exchange rates as a key barrier, which might be overcome by microbubble dispersions. Microbubbles that start out small and do not coalesce are a special feature of FO generation, but generally, surfactants stabilise the size distribution by the colloidal effect that induced charges from surfactants repel approaching microbubbles. Hence, even with substantially higher surface areas per unit volume, the surfactant blockage (α-factor) and small driving force for mass transfer to the liquid pose very small mass transfer rates. This barrier should hold for dosing of nutrient gases but also for stripping of product gases. The idealised scenario in **Figure 1(d)** suggests that with nearly insoluble gases, the collision mechanism for direct microbe, microbubble gas exchange should become the dominant mechanism for dosing or stripping.

The evidence that speaks to this is from Al-Mashhadani *et al.* (26), who introduced ~550 µm (see next section for bubble size distribution) microbubbles in an airlift loop bioreactor for staging AD of wet food waste. The reported control was an unbubbled anaerobic digester, but the case of an identical fine bubble dispersion system, no FO, resulting in 1–4 mm diameter microbubbles, was reported by Al-Mashhadani (27), all using the same batch of prepared wet food waste and sludge inoculant. Of the bubbled systems, 5 min per day of dosing or stripping was conducted. This double control system showed that there was a modest increase in methane production rate for the no FO, but bubbled system (see **Figure 3**), which increased with increasing CO_2 composition in the fine bubble. Al-Mashhadani *et al.* (26) reported a doubling of the production rate with microbubbles, all the methane removed from 20–25 days in the control of no bubbling was equivalent to the FO stripping (at 5 min per day dosing and stripping) in 10–12 days. But with FO generated microbubbles, the production rate of methane more than doubled, stripping with pure CO_2 microbubbles. Sensitivity experiments showed lengthening the stripping or dosing interval beyond 5 min per day made no difference to the amount of methane removed.

Why this is troubling, however, has to do with observations made by Al-Mashhadani *et al.* (28) of K_La for the same airlift loop system with aqueous media, without fermentation broth, metabolic digestion products or AD microbial consortia, the purely physicochemical hydrodynamics problem of mass transfer. The conclusion was that both O_2 and CO_2 dosing or stripping could be conducted to the saturation limit or in the case of using nitrogen as the stripping gas, to trace levels of the dissolved gases. Using FO had the effect of greater K_La over fine bubble mediation, as greater energy efficiency, but the endpoints were identically achievable. So both AD systems, microbubble and fine bubble dosing or stripping with pure CO_2 composition, achieved dosing of CO_2 to saturation and stripping of all the available dissolved methane, in the 5 min per day of sparging. The mass transfer rates

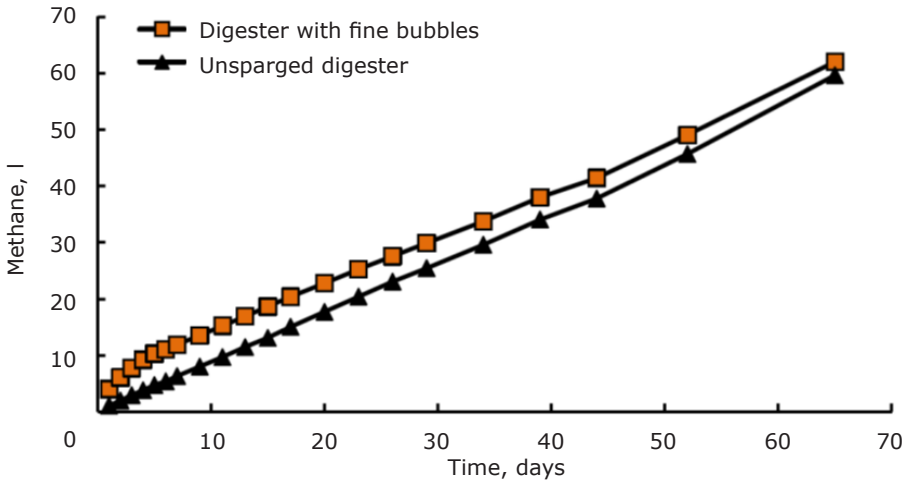

Fig. 3. Cumulative methane volume collected from the fine bubble ALB and control of no bubbling ALB with anaerobic digestion of wet food waste (27)

inferred from K_La were significantly higher than the metabolism of the AD consortium. Relative to the slow metabolism, more rapid stripping and dosing are superfluous. Yet modest increase with fine bubbles, but doubling with microbubbles, is inexplicable with the removal of the inhibition effect of methane alone, both digesters strip the available methane. So why was so much more produced on every daily cycle when microbubbles were seeded?

Figure 1(c) only accounts for an increase in K_La due to collisions with microbubbles and insoluble gases. But K_La increase does not change the endpoint of methane stripped nor CO_2 saturation, as both are achieved in the fine bubble and microbubble sparging cases. This mystery was not reported explicitly in the literature, due to no viable hypotheses to explain it at the time of publication (26). The next subsection introduces a third competing mechanism for gas exchange in fermenters.

2.2.3 Microbes Coordinated on Microbubble Interfaces

Figure 1(c) shows that collisions can remove the nearly insoluble gas layer surrounding the microbe that secreted it as an extracellular metabolite. Stripping a product from the vicinity of the microorganism that produced it reduces inhibition, so increases metabolism. But since fine bubbles can also strip out the same extracellular metabolite dissolved gas, the doubling of methane production rate is inexplicable if the same condition exists after either fine bubble or microbubble stripping of methane (26). Logically, a difference must exist for the different outcome.

There are two clues about the different state that exists in the airlift loop bioreactor (ALB) for AD of wet food waste described by Al-Mashhadani *et al.* (26, 27) for microbubble and fine bubble stripping with pure CO_2 sparging. **Figure 4** (27) shows the estimated bubble size distribution from image analysis. There is a very small population of sub-100 µm microbubbles with that particular ceramic diffuser system, as inferred from image analysis. Desai *et al.* (29), however, showed from ABS that smaller bubbles are hidden behind larger bubbles using image analysis, so there is a strong likelihood of a small, but significant population of sub-100 µm microbubbles in the AD scenarios reported. Of that microbubble population, 20 µm size microbubbles rise so slowly that they would be expected to be retained within a metre-height vessel the next day. Indeed, our earliest uses of ABS in a tank with greater than one metre water height reused the water by nitrogen stripping for aeration mass transfer studies with membrane slit diffusers. Anecdotally, as soon as our hydrophones with lowest resolution of 20 µm were introduced into the tank and ABS began, a spike at 20 µm was all the bubble size population reported. This was with higher void fraction than what would be expected in an existing system. Fan *et al.* (4) refer to this phenomenon of entrained microbubbles that are long-lived due to the combination of the inertia of residual liquid currents and small buoyant force as a 'bubble bank'. Desai *et al.* (16) showed the average 7 µm size microbubbles could readily be produced using an alumina ceramic diffuser with hydrophilic pores, incorporating a resonant mode by tuning the amplitude and frequency of FO. It further showcased how the smallest sized microbubble could be generated in a given set of orifices. Such bubble clouds not only achieve, to the equilibrium level, dosing and stripping of dissolved gases, but maintain a long-lived presence of the bubble bank within the vessel. Computational fluid dynamic simulations by Al-Mashhadani *et al.* (3) show that within these ALBs, sub-100 µm microbubbles remain entrained indefinitely; subject, of course, to the modelling idealisations of monodispersity and non-coalescence.

So what are the implications of the bubble bank identified in the AD and ALB studies of Al-Mashhadani and coworkers? Embedded, dispersed bubble bank with sub-100 µm diameter are likely to collide with microbes on a regular basis. Many microbes, however, have amphoteric character that attracts them to bubble interfaces. In the next section, absorptive microbubble separation bioprocesses are reviewed, showing the widespread observation of microbubble-microorganism attachment, including tailoring solution chemistry to form flocs for flotation separations.

Figure 1(d) depicts a complex of microbubbles with microbes, which provides a direct release for the microbe of an extracellular metabolite gas, immediately diluted into the microbubble. It follows that insoluble gases have an immediate exit route from the vicinity of the microbe producing them. The diffusion coefficient of solutes in liquids is typically $\sim 10^{-9}$ m^2 s^{-1}. By contrast, the diffusion coefficient of solutes in gases is typically $\sim 10^{-5}$ m^2 s^{-1}. Consequently, the inhibition effect without the daily seeding of microbubbles for extracellular metabolite insoluble gases builds up a gas-rich layer

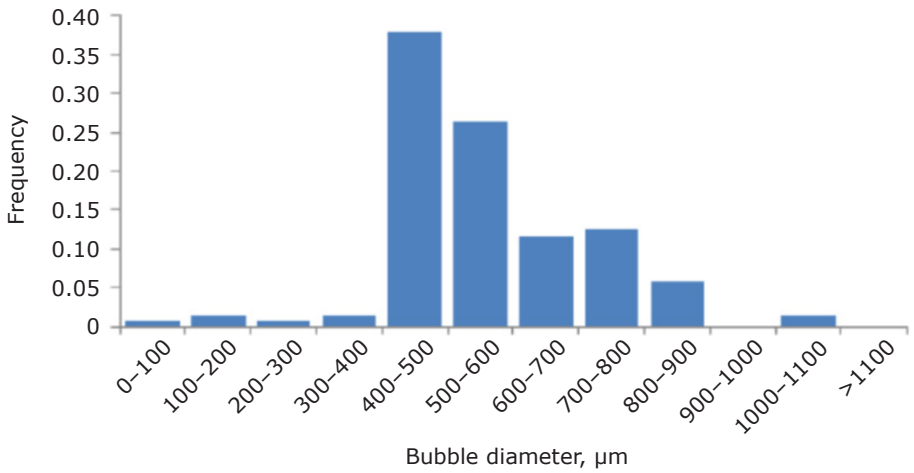

Fig. 4. Histogram of bubble size frequencies estimated by Al-Mashhdani (27) using image analysis with clear water medium

around microorganisms throughout the day, in the scenario of AD and ALB studies with fine bubble mediated gas exchange. That small population of sub-100 μm microbubbles in the bubble bank provides a potential mechanism for the removal of methane by such complexes of microbubbles and microorganisms.

One of the authors spent an afternoon during the multi-year study reported by Al-Mashhadani (27) watching both the ALB with FO and that without, which were stagnant due to the 5 min per day of sparging scheduled first thing in the morning. He observed that in the ALB that had been sparged with oscillatory flow, bubbles would grow, seemingly trapped by the biomass, until it was coarse bubble size (~1 cm diameter), certainly visible. Eventually the bubble would break off, rise to the liquid surface with the headspace, and burst. This occurrence was frequent with the microbubble ALB, but much less frequent with the ALB that had been sparged by steady flow. The mechanism could be described as the microbubbles seeded in the bubble bank provide local 'life rafts' for the microorganisms, with an easy route for methane removal across the gas liquid interface, that eventually grow to be 'supertankers' that traverse the bulk liquid to leave their cargo at the headspace 'port'.

Throughout this section, **Figure 1** might give the impression that microbubbles are spherical, and that the spherical shape imposes mass transfer limitations due to the spherical shell of the diffusion boundary layer. Actually, microbubbles that become surfactant laden on the interface, such as those used for medical imaging and drug delivery (30) which are stabilised by lipid encapsulation have rigid interfaces and only deform with external resonant forces, such as ultrasound.

Before the microbubble interface becomes immobilised and blocked by surfactants, as posited by Clift *et al.* (10), there is an opportunity for rapid mass transfer such as gas exchange with dissolved gases in the liquid. Zimmerman *et al.* (31) mooted that the time scale for homogenisation or equilibration between the interior of the microbubble and the liquid on the interface is a few milliseconds for ~100 μm sized bubbles. Desai *et al.* (6) reinforced this assertion with stripping of ammonia by microbubbles of that scale with thin liquid layer heights enforcing such contact times, demonstrating very high K_La values. One potential mechanism contributing to these high values are the shape oscillations of microbubbles just after detachment, which are shown by Tesař (32) to occur within a few milliseconds. These shape oscillations provide highly convective flow through liquid boundary layer. A crude estimate is that rising microbubbles are likely to become saturated with surfactants on the time scale of tenths of seconds, inferred from adsorption studies on 1.3–1.5 mm fine bubbles by Krzan *et al.* (33) for *n*-alkanol solutions. Obviously, the characteristic time scale for adsorption of interfaces is strongly dependent on liquid composition and may well depend on microbubble size and other conditions of the solution.

What distinguishes the collision and release of **Figure 1(c)** and collide, stick and form complex **Figure 1(d)** is the lifetime of the 'collision', where the latter ends with the bubble bursting. If the collision and release mechanism were dominate, it would take a large number of collisions to collect that substantially higher volume of methane produced than the fine bubble sparging case. One way to test the hypothesis underpinning the 'collide, stick and form microbubble-microbe complex' mechanism is to increase the population density of non-buoyant microbubbles forming the dispersed bubble bank, but with smaller bubble size on average, such as tuned by frequency of oscillation by Desai *et al.* (16). Such microbubbles

would have insufficient buoyant force to deviate from liquid currents, which are very stagnant without sparging, so hydrodynamic collision theory would lead to low collision rates, and thus a modest increase in methane production rate according to the collide and release mechanism hypothesis. Evidence to support this hypothesis will be explored in Section 4.

3. Absorptive Microbubble Separation Methods for Bioprocessing

Downstream processing innovation is essential for the development of sustainable industrial biotechnology, as the methods commonly used for high-value added bioproducts, for example centrifugation, preparative high pressure liquid chromatography, flow cytometry for cell sorting and electrophoresis, do not scale up to industrial commodity chemical throughputs very well. These methods are either too expensive if multiplexed or unable to deal with large liquid volumes in larger vessels. The candidate technologies that do scale well, for example filtration, liquid-liquid extraction, absorptive bubble separation, fractional distillation, selective membrane separations and ion exchange, to name a few classes, need to be tailored or creatively adapted, for the chemical and physical complexity of bioproduct mixtures. Microbubbles can mediate either the tailoring or creative adaption. In this section, the various classes of absorptive bubble separations are reviewed, with the role of microbubble mediation explored.

Figure 5 shows a classification of absorptive bubble separation processes. Central to an absorptive bubble separation is the extent to which a surfactant can be loaded on a gas-liquid interface, and then the chemical configuration of how the species is absorbed. Chemical thermodynamics yields one key relationship at equilibrium, the partition coefficient K, which is the ratio of concentration on the bubble interface to the concentration in the bulk. Conventionally, absorbed surface concentrations are reported in moles per unit surface area of the dispersed phase, so K has the units of cm^{-1} in typical centimetre-gram-second metric units. At equilibrium, it should be noted that the interfacial tension γ is the Gibbs free energy per unit surface area, so the partition coefficient can be expressed through the Gibbs equation as Equation (xi):

$$K = -\frac{1}{RT}\frac{d\gamma}{dC} \quad \text{(xi)}$$

Interfacial tension in aqueous solution is known to be highly sensitive to contamination, so selective absorption is possible with the partition coefficient large in the region of high surface tension drop due to surfactants preferentially attracted to and loading bubble interfaces. Typically, the change in surface tension is affected by micelle formation along the bubble interface, where high surfactant concentration is credited with coordination of surfactants in the nearby bulk liquid, stabilising

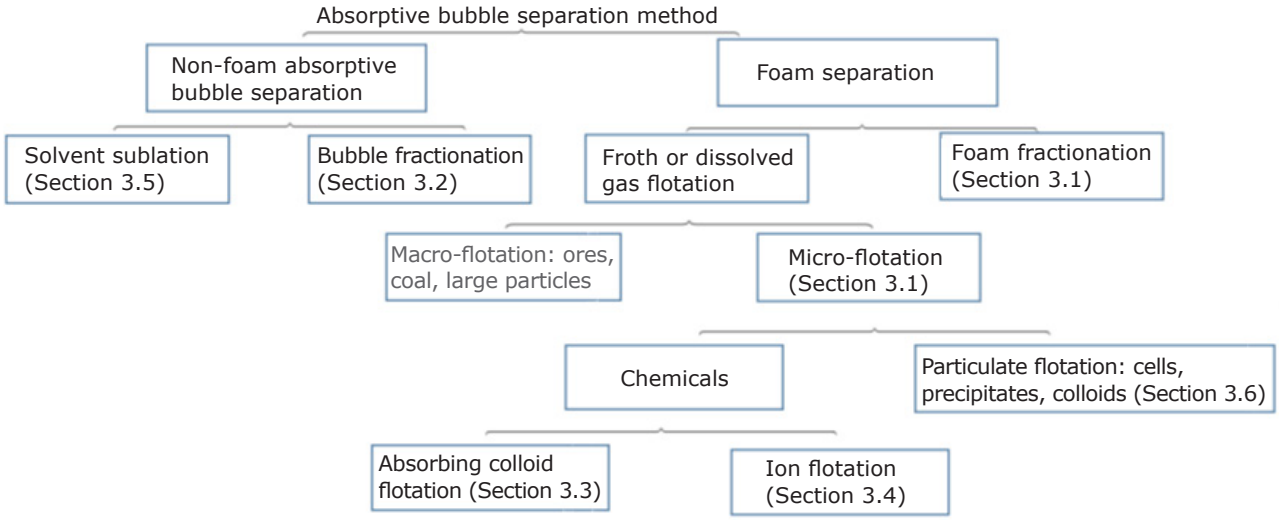

Fig. 5. Schematic classification of adsorptive bubble separation methods. The signposts on the schematic are the subsections of the present article where the approach, particularly as adapted to microbubble mediated bioprocessing, is treated. Macro-flotation is not treated in this article (greyed out) due to the lack of microbubble usage and no current bioprocessing applications

the nascent micelles (34). The earliest class of microbubbles, used for ultrasound contrast agents for medical imaging, are surfactant stabilised for longevity due to this absorption effect (35).

All of the bubble mediated processes presented in **Figure 5** are intensified by microbubbles, at least in the pedestrian sense due to much greater surface area per unit of gas volume. However, mechanistically, microbubble mediated absorption dynamics potentially benefits from the greater coordination effect exposed by molecular dynamics simulations for micellar adherence to the interfacial surfactant layer, increasing speed of uptake and surfactant loading (34) at equilibrium.

Another physicochemical effect that can influence attraction of ions, molecules and particulates to microbubbles is charge. Takahashi (36) demonstrated that the zeta potential of air microbubbles in water indicates a negative charge. Ionic strength has a well-known stabilisation effect on microbubbles, results in smaller average bubble size due to the opposition to bubble coalescence, and therefore leads to greater ion complexation in the interfacial region of microbubbles (37).

Physicochemical hydrodynamics of bubble-particle collisions are strongly influenced by pH, surfactant and ionic strength, not least through their effects on particle zeta potential, as well as the relative size of particles (38). In particular, bubbles and particles that are within a factor of 10 in the ratio of diameters have a substantial collision cross-section, hence a stronger possibility of forming flocs. As microbubbles load greater surfactant, ion and charge interfacial content, these collisions are likely to be 'stickier' than with larger bubbles and particles. Bubble size with microbubbles, therefore, allows for greater tuneability for selective separations.

These enhancement mechanisms, along with others, for microbubble mediated absorptive separations, will be explored among the classes of separations identified in **Figure 5**. Particular attention will be paid to the potential for downstream bioprocessing within these classes.

3.1 Microflotation

Colloidal particle separation from an aqueous solution is difficult for membranes and filtration processing, due to the small size of the particles. Flotation processes exploit the key mechanism by generating microbubbles of the appropriate size distribution that attach to hydrophobic particles. Resultant flocs are more buoyant than the surrounding liquid, so rise to the surface of the flotation cell. In froth or foam flotation, the overspill of foam is collected to harvest the particles. In dispersed or dissolved gas flotation, bubble rupture accumulates the particles that can be recovered from skimming the top surface (39).

Recovery of valuable end-products is the goal in flotation separation. The most common harvesting bioprocess uses DAF for removing microalgae and other small particulate matter in the first stage of potable water purification, where raw water is sourced from lakes, rivers and estuaries (38, 40). Recovery of the microalgae by DAF is long established for high-value added constituents such as beta carotene (41, 42).

Microbubbles generated by FO have been used to float, dewater and harvest microalgae (14), separate oil droplet emulsions in water (43) and yeast harvesting post propagation (44). Hanotu *et al.* (14) argue that due to much lower exit nozzle velocities than DAF, microbubble flotation by FO uses one thousandth relative power density. However, the saturation-nucleation mechanism for microbubble formation is not the most power consumptive feature of DAF. Large liquid pumps overcoming 6 bar pressure generated by the saturator are the most power consumptive. By comparison, the air flow generated to feed the fluidic circuitry is the most power consumptive feature with FO generated microbubbles.

'DZ microflotation' was developed to reduce costs in flotation using a combination of FO derived microbubble generation and flocculation methodology. These reduce operating costs significantly, with approximately 90% total savings possible in an operating environment with several fold greater performance in the form of microbubble throughput of required size. Using laminar generated microbubbles has led to higher levels of floc formation, with concomitant reduced floc destruction. The use of specific gases and strategies for floc formation relying on wettability in the gas-liquid and solid phase results in the third combination which directs the bubbles and makes them 'stickier'. Since bubble size is controllable (16), performance is easily improved upon existing DAF systems, and provides significant control and manoeuvrability. In fact, many DAF systems face challenges due to reduced floc stability due to temperature variations whereas DZ microflotation can overcome this using different gases and the bubble bank approach injected in a laminar fashion.

There are other advantages aside from the potentially nearly 90% operating cost reduction.

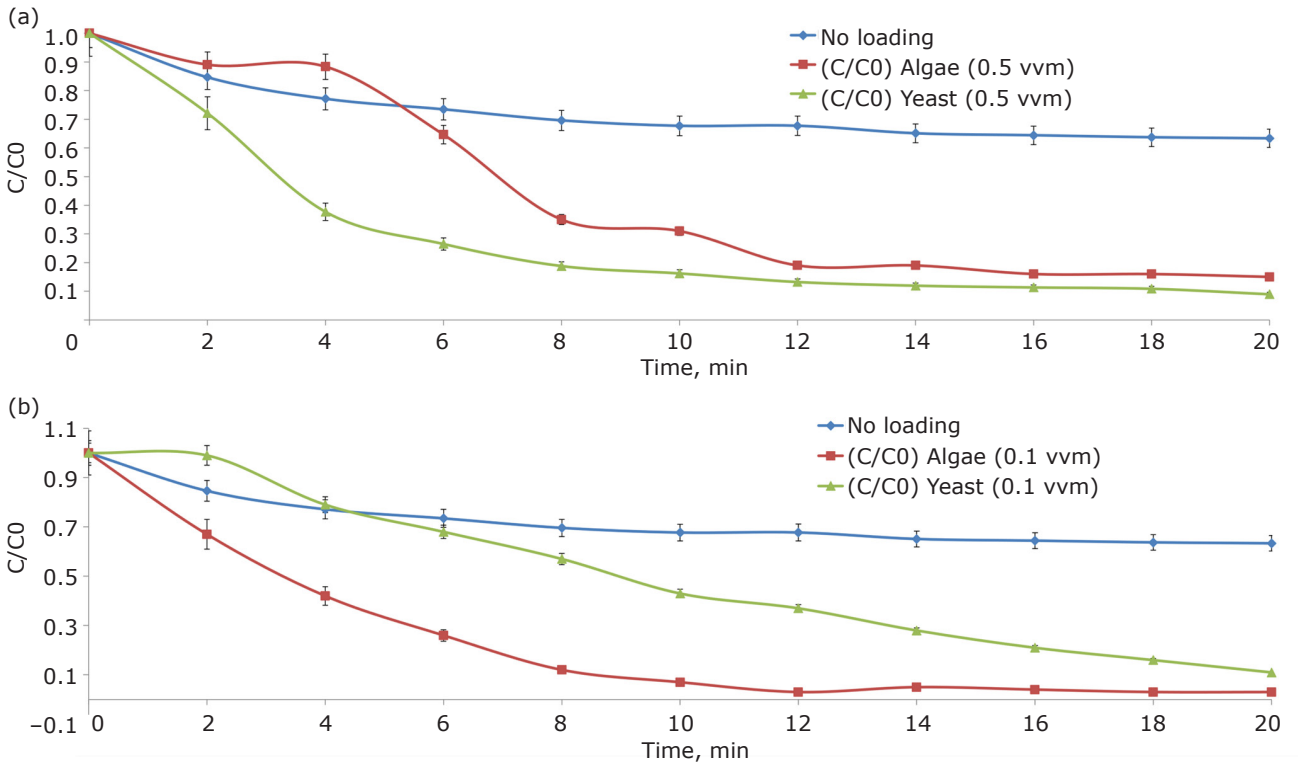

Fig. 6. DZ Microflotation used for selective separation for yeast (*S. cerevisiae*) from microalgae consortium. Concentration *c* for yeast and for a mixed consortia of microalgae are inferred from optical density with different wavenumbers. c_0 refers to the optical density at the initial time. No loading refers to the fermentation broth used for the co-culture without the addition of the microorganisms

The multiple-fold improvement in bubble flux, and process versatility and control. This comes in the form of a substantially lower capital cost and insurance risk. Typically, one of the major costs in a DAF system is the insurance liability due to requiring operation at higher pressures. This is immediately removed as the liquid is now operating under ambient pressure. To summarise, DZ microflotation does not require capital intensive saturation, liquid recycle or large pumps rated for 6 bar, and achieves a faster separation cycle than conventional DAF due to the greater success rate of bubble attachment for floc formulation in laminar flow.

Figure 6 shows the selective separation performance of the DZ microflotation applied in the flow cell for different flow rates relative to the flow cell volume (0.1 vvm and 0.5 vvm). The microbubble sparging removes some volatile organic compounds that change the opacity and could oxygenate some components. Hence the no-loading time trace serves as a control experiment for the selective flotation, as well as a benchmark for calibration for the solution with yeast and the mixed microalgae consortium. The experiments were repeated but as transient experiments do not quite have a unique zero of time definable, so the behavioural trends are the same. Selective points had limited repeatability towards 18–20 min and the error bars have not been included there. The selective flotation is of a consortia of microalgal strains which included *Nannochloropsis, Chlorella, Dunaliella* and *Tetraselmis* genuses. Yeast is the common strain *Saccharomyces cerevisiae*. The graphs show the achievement of remarkably distinct selective separation based on residence time and flowrate. Additionally, no flocculent was used for this separation. 0.1 vvm and 8–10 min residence time achieves ~7:1 selectivity for yeast, whereas 0.5 vvm and 6 min residence time achieves the reverse selectivity of >2:1 for microalgae recovery.

Generally, in froth and foam flotation, the selectivity among different types of particulates occurs due to the tailoring of the combination of pH, flocculants and coagulants to achieve a solid surface zeta potential that is hydrophobic, presuming the air bubbles and aqueous solution (45). The point of zero charge for any particular solid particulate species is different, so that conditions can be chosen so that preferentially one of the two particulate species is hydrophobic

and the other hydrophilic, hence one species is floated and the other stays dispersed in the liquid phase. With DZ microflotation, the attraction to the microbubble phase changes with volumetric flowrate due to size difference, which influences the bubble size distribution and phase fraction, as shown in **Figure 6**. Staging and tailoring segregation requires no compositional change to the liquid medium, at least in this instance.

Studies have been carried out with bacterial and algal systems, insect larvae and talc of different sizes, achieving selective flotation segregation. As this was a preliminary study, whether it holds more widely than these classes of separations from would be promising to explore. Each system has multiple control handles due to the properties of the microbubble phase being controllable, particularly narrow bubble size distributions with gas compositions tuned.

In terms of foam flotation, a novel separation technique which utilised stable microbubble structures, described in features below, was developed on the basis of surface tension, exploiting the following features:

- Typically a frother is required for foam flotation but for liquids with a high level of surfactants already present, such as leachate, digestate, centrate, fermentation broth, it is not needed
- Foam is formed when the bubble hits the top surface and cannot escape due to the surfactant stabilisation
- As per the Young-Laplace equation, the smaller the bubble, higher is the surface tension balancing the Laplace overpressure
- Basic principle of nanotechnology is smaller building blocks make for more robust structures due to reduced voidage (46)
- The same holds true for foams. The smaller bubbles stabilise the structure and tend to also not breakthrough the surface due to a combination of low rise velocity (Stokes' rise equation) of the smaller bubbles and higher stability of the new foam structure (47)
- These microbubbles can be made to stabilise and destabilise foams, by using variable gas with bubbles of different sizes, or by using the correct combination of gas and frother, if necessary (48)
- The foam structure is now stable and a similar approach as discussed in the above sections can be undertaken for optimal separation.

Figure 7 shows that variation of pH has a dramatic effect on talc recovery from aqueous solution, achieving sensitivity greater in dynamic range than a benchmark study for talc foam flotation (49). Talc tends to have a hydrophilic surface on the edge and hydrophobic surface on the face when it breaks. The preliminary study shown here does not vary the key processing variable, contact time, from 10 min, nor does it add foaming agents, coagulant or flocculants to vary the zeta potential.

Typical foam flotation depends on the frother concentration which dictates the foam stability formed and the subsequent flotation that occurs. This shows a direct dependence on the frother concentration to the flotation efficiency. Where this

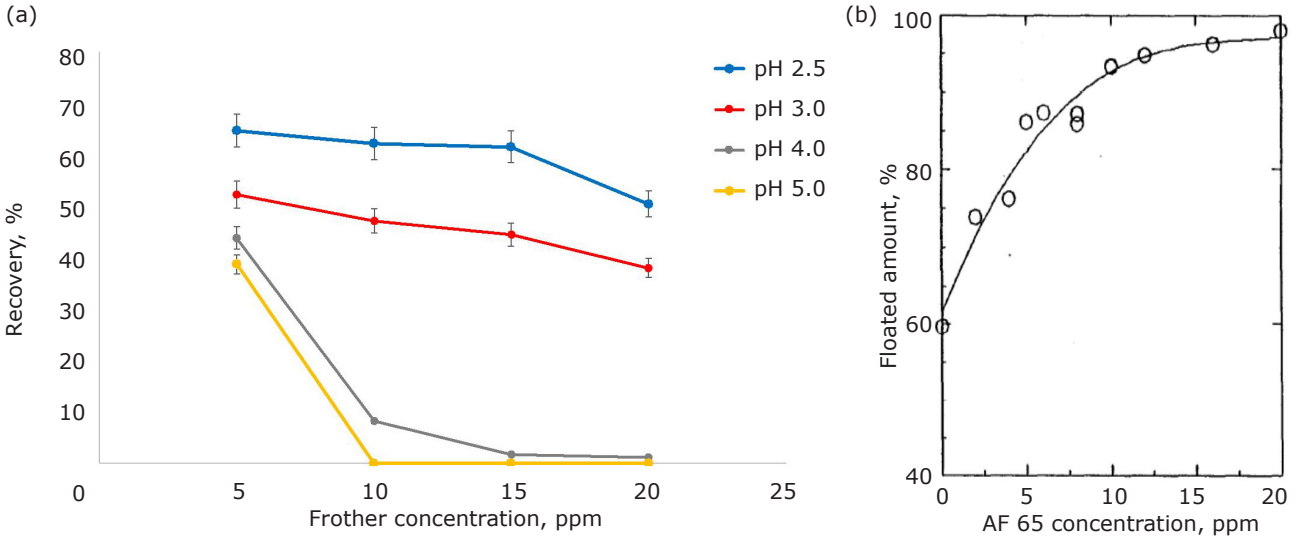

Fig. 7. Comparison of: (a) present article approach for foam flotation approach; with (b) Yehia and Wakeel (49). Flowrate is 0.1 vvm with processing time set at 10 min

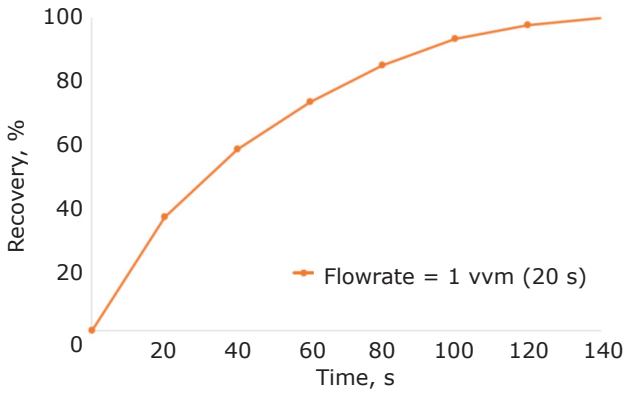

Fig. 8. Talc recovery efficiency from aqueous solution with foam build in an initial 20 s duration with 1 vvm volumetric flow rate (not shown) followed by a second stage of no sparging

novel foam flotation approach differs is that the foam is inherently stable even at a lower surfactant concentration, and hence additional frother is unnecessary. Similarly sized monodispersed bubbles would offer stability due to reduced Ostwald ripening which is one of the factors on which the foam floatation approach follows. With reduced surfactant concentration, microbubble stability is reduced, but the mechanism described above ensures adequate stability. The difference in the performance and the effect of the microbubble foam flotation approach ensures that the bubbles are able to reduce the dependence on the frother as the foam stability is already higher.

When flotation flow rate is increased for the novel foam flotation approach to 1 vvm for 20 s and switched off to appropriately test the hypothesis of the foam build, 70% separation occurs at 20 s, and >97% separation occurs within 120 s (see **Figure 8**). The experiments were repeated but as transient experiments do not quite have a unique zero of time definable, so the behavioural trends are the same. This demonstrates a chemical cost significant saving (~9.7%) over conventional approaches and even microbubble-based approaches for coal flotation type systems which require at least 75 vvm of gas flow and 12 min of processing (50). Coal flotation systems are excellent indicators and comparators with talc flotation due to similar properties (hydrophobic surface) and systems requirements.

Gilmour and Zimmerman (1) discuss the DAL/DMS approach, which is further explored in Section 4 of this article. DAL/DMS has significant ramifications in bioprocessing, production, *in situ* product removal and downstream separation whilst enhancing bioreactor production rates, in some cases by orders of magnitude. For instance, DAL/DMS and novel foam flotation or DZ microflotation can then be used to develop a one pot bioreactor for production of microbial or microalgal systems and subsequent separation as seen in the industrial work performed at Reepel Ltd, UK, which is developing microalgal bioreactors which can increase production rate (biomass), biologics (which can be separated in an *in situ* manner), solid biomass separation using DZ flotation and disinfection or lysing using advanced oxidation microbubbles. A single bioreactor capable of achieving these features whilst reducing total expenditure (TOTEX) by 85% is a step change in bioreactor systems.

One of the important outcomes was the ability to separate a consortium of algal systems which were used to treat oil-based wastewater and separate both the algae and the oil out leaving a clear, transparent liquid. This work is soon to be published but one output is seen in **Figure 9**. The liquid at 0 min mark in **Figure 9(b)** is lighter than the bottle shown below as the majority of the oil was separated within seconds of being placed in the flotation column. The final sample in **Figure 9(c)** was clean enough to be sent to municipal sewerage.

3.2 Bubble Fractionation

Closely aligned with microflotation of particulates is bubble fractionation. With bubble fractionation, gas bubbles travel through a long column, typically, of the bulk aqueous phase, transporting surface active material to the top of the column (51). Lemlich (51) developed a theory based on gas absorption and bubble rise or convection for the preferential concentrating of the absorbed species at the top of the bubble column. Fields *et al.* (52) showed with absorbed bacteria that fitting a Langmuir-type isotherm works very well against experimental performance data. From observation of microbubbles rising, the separation into riser and downcomer regions occurs, regardless of whether there is an internal baffle, such as in an airlift loop bioreactor, so that the riser region is actually well mixed (3). This would explain why the Langmuir-like isotherm fitting works so well, rather than a distributed system model such as deployed by Lemlich (51). Similarly, Suzuki *et al.* (53) found that Langmuir-type isotherms described the fractionation of humic acid and crystal violet in a bubble column very well.

To the authors' knowledge, there is no published study of nonfoaming microbubble foam fractionation

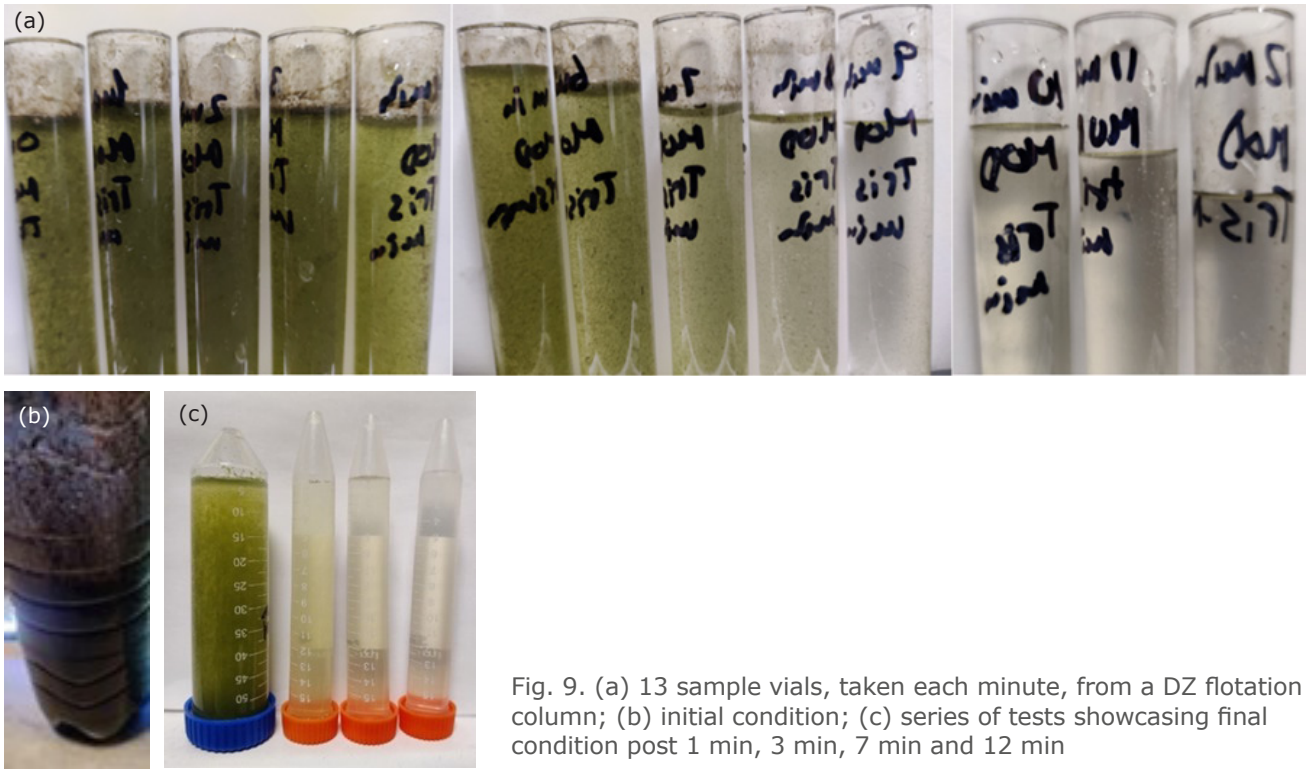

Fig. 9. (a) 13 sample vials, taken each minute, from a DZ flotation column; (b) initial condition; (c) series of tests showcasing final condition post 1 min, 3 min, 7 min and 12 min

of chemical species for absorption. There are two unpublished studies that the authors have participated in, both for the absorption-desorption dynamics of CO_2 comprising microbubbles in: (a) ionic liquids; (b) monoethanolamine (MEA). The first ever blowing of bubbles (and microbubbles) into ionic liquids was shown by Taylor *et al.* (54). Subsequently, thin layers of ionic liquids were systematically used to scrub CO_2-rich microbubbles, absorbing CO_2 exothermally, and then hot CO_2 microbubbles were used to strip CO_2, desorbing CO_2 endothermically. In both cases, the temperature of the liquid layer barely changed. This exploits an analogous feature of evaporation dynamics of hot microbubbles first observed by Zimmerman *et al.* (31). The heat of vaporisation of a volatile liquid is removed from the microbubble at its interface, therefore providing a cool layer that opposes heat transfer from or to the microbubble. This is known as the Leidenfrost effect (55). Desai *et al.* (56) show that this Leidenfrost-like effect achieves zero lysed cells, as the collisions between hot microbubbles and cells or microorganisms are protected by the Leidenfrost boundary layer of the microbubble. In fact, subsequent studies indicated an increase in cell viability for bacterial systems due to the enhanced effects of DAL/DMS.

Combined with the notoriously slow heat transfer through the laminar boundary layers surrounding a rising microbubble, the rate of heat transfer is very slow, allowing the liquid to remain nearly isothermal, even with ~100°C temperature difference (57). In the case of exothermic absorption, this allows the heat of absorption to leave with the microbubble as it bursts at the top surface of the liquid layer, releasing the heat in the vapour phase. The benefit of maintaining the liquid as nearly isothermal is simply the solubility of CO_2 in carbon capture liquids is temperature dependent, decreasing with increasing temperature. Hence, ordinary CO_2 absorption heats the liquid, opposing more absorption by decreasing the chemical thermodynamic driving force. Microbubble mediation, however, maintains the driving force as the solubility limit, but with the additional benefit of the bubble bank wherein some microbubbles can be engineered to remain entrained in solution, thereby providing a supersaturation at atmospheric pressure. This property is only useful for transient operations to ensure that higher loading capacities are achieved prior to desorption. The entrained bubbles have been observed in biological systems and we are exploring these in chemical and biological processes (4).

Figure 10 shows the amount of CO_2 absorbed by an MEA 30 wt% solution used as an industrial comparator. The average bubble size is 190 μm. The contactor has an adjustable 700 ml volume; gas throughput is maintained approximately at 0.5 vvm ± 5% (when recycled through) due to

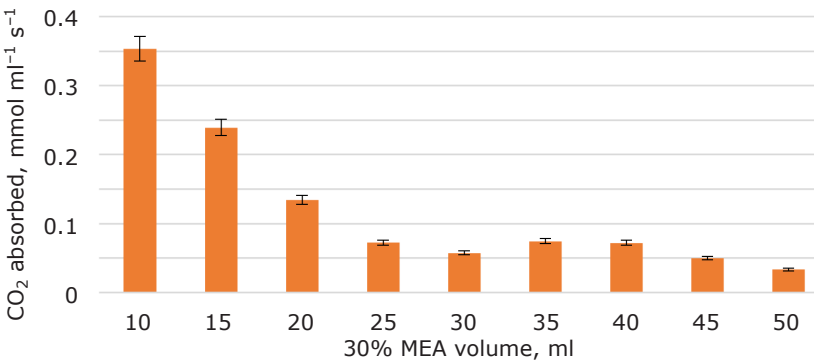

Fig. 10. Concentration of CO_2 absorbed in 30% MEA in the microbubble contactor of Desai *et al.* (6) from zero in 30 s of microbubbling with pure CO_2 microbubbles

low flow rates and minor variations in density and viscosity. The saturation loading of CO_2 is 0.5 mol_{CO2} mol_{MEA}^{-1}. For 700 ml volume, loading time is shorter with the microbubble contactor (6) by 40%, approximately 0.06 mol_{CO2} mol_{MEA}^{-1} more loading with the microbubble contactor than without. With the same short contacting time of 30%, more than seven-fold increase at 10 ml (low liquid layer height) than the five-fold higher liquid layer height.

The desorption dynamics of CO_2 from CO_2-saturated carbon capture liquids would appear, superficially, to be impossible, as there is no concentration driving force. However, the driving force is actually the chemical activity difference between the phases, and the fugacity of CO_2 at high temperatures, in the bubble phase, is significantly lower than CO_2 absorbed in carbon capture liquids at low temperatures. This is illustrated by a Langmuir-type rate law for the absorptive/desorptive flux, introduced originally for non-equilibrium microbubble mediated separations of ethanol-water (22) and of ammonia-water solutions (6), Equation (xii):

$$\dot{n}_i = k_i A(x_i \gamma_i P_i^* - P_i) \quad \text{(xii)}$$

The left hand side of Equation (xii) is the molar exchange rate of species i (just CO_2 in this case); k_i is the component Langmuir-type collision coefficient; A is the surface area of the microbubble phase; x_i is the mole fraction of the species in the liquid phase; γ_i is the activity coefficient; P_i^* (T_g) is the saturation pressure at the temperature in the microbubble phase; P_i is the partial pressure in the microbubble phase. The right hand side of Equation (xii), if set to zero (equivalent to no net exchange of species across the microbubble interface), is the generalised Raoult Law. Hence, the driver for mass transfer is the difference from equality of the Raoult terms.

The point here is that P_i^* (T_g) for CO_2 at temperatures well above its boiling point can be very large, due to the Clausius-Clapeyron Equation (xiii) for the vapor pressure P^* at temperature T growing exponentially:

$$\frac{P^*}{1\ \text{atm}} = \exp\left[\frac{\Delta H_{vap}}{R}\left(\frac{1}{T_b} - \frac{1}{T}\right)\right] \quad \text{(xiii)}$$

with T_b = −78.46°C and ΔH_{vap} = 16.4 kJ mol^{-1} at 100°C; P^* = 127 atm. Consequently, the first term on the right hand side of Equation (xii) even at very low mole fractions of CO_2 absorbed in the carbon capture liquid, which maintains low temperatures with low liquid layer heights, yet ~100°C microbubbles. Hence, microbubbles can provide temperature swing for absorption (carbon capture) and desorption (regeneration) with negligible heating and cooling of the carbon capture liquid.

So how effective is the hot microbubble desorption process, the same approach as **Figure 10** but with CO_2 saturated MEA and hot, pure CO_2 microbubbles? A weak chemical thermodynamic driver was trialled with 80°C gas temperature and liquid temperature at 60°C. Complete desorption in 7 min of contacting occurred. The industrial processes as a benchmark require 140°C and 2 bar pressure.

3.3 Colloid Flotation

Lemlich (58) introduced the theory, models and experimental findings of precipitate and absorbing colloid flotation. A review of the standard industrial practice was prepared by Clarke and Wilson (59). In general, these related technologies are preferred for removal of inorganics from aqueous solution over ion flotation and foam fractionation due to the ability of the precipitate and absorbed colloids either to produce surfactants or complex *via* surfactant effect at bubble interfaces. Alexandrova and Grigorov (60) demonstrated the effectiveness

of these combined approaches for removal of dissolved metal ions (copper, lead and zinc) from aqueous solution. Minerals engineering applications typically follow the approach of changing pH to precipitate the ions as salts, adding flocculants and coagulants to form colloids, that are tailored as well to make the colloid zeta potential sufficiently hydrophobic to attract and absorb the colloids as a floc that is floated. Jameson and jet cells are both effective at conducting currents to increase collision efficiency and therefore recovery rates (61).

A related approach was adopted by Pooja *et al.* (62) who considered the use of biosorbents to absorb toxic, heavy metal ions and then flotation of the biosorbents, which are often cheap biomass that is readily harvested with even large bubbles. The approach, however, is non-selective and creates more toxic waste, unless the biomatter is microbial or microalgal that uptakes specific heavy metals in their metabolism. With such microscale uptake, there are challenges in collecting the microparticles. The benefit, however, is the densification of the waste material into small, manageable volumes. Microalgae that are cultivated for bioproducts rarely achieve higher concentrations than 10 mg l^{-1} (19). Harvested and dewatered, such microalgal biomass achieves densities on the order of >1 kg l^{-1}. Storage of such toxic waste is much more compact.

Likewise, nutrient recovery is possible using a combination of engineered consortia and microbubble bioreactors used for production and downstream separation. This helps recover nutrients from waste streams which would otherwise be sent for treatment. Concentrating these nutrients and utilising engineered microalgal consortia can provide several benefits which include:

- CO_2 sequestration of the order of nearly 1.8–2 kg per kilogram of algal biomass produced
- Concentrated nutrients recovered from waste streams reduces indirect emissions
- These engineered consortia which now have concentrated nutrients form an excellent fertiliser with higher bioavailability and performance for crops and the soil.

Combination of technologies utilised for ammonia recovery in waste streams (6) and microalgal recovery of additional nutrients with or without concomitant CO_2 sequestration has been developed and scaled for various scenarios.

One would think that the greater surface area of microbubbles would enhance such processes. Microbubbles can carry charge. This has long been exploited using a class of microbubbles called colloidal gas aphrons (CGAs). Fine particulates are difficult to separate using conventional minerals engineering approaches, so microbubbles that are of the same order of size are much more likely to collide with fine particles. The concern, however, is that conventional microbubbles may not adhere as well with fine particles, due to the typical high power required to form microbubbles creating turbulent shear, which opposes floc formation. CGAs are typically generated by high-speed impellers, hence strongly turbulent eddies are generated, but with anionic surfactants that lead to charge loading on the microbubble interface. Manipulating the zeta potential with pH then allows microbubbles to collect oppositely charged fine particles (63).

Whether or not charging microbubbles is necessary is brought into question with FO generated microbubbles. Hanotu *et al.* (14) demonstrate much lower exit nozzle velocities than DAF, estimated that the process can be maintained entirely in laminar flow conditions. Conventional wisdom has always been that turbulence enhances flotation separation performance. Hanotu *et al.*'s (14) proof-of-concept, laboratory bench experiment did not actually achieve bubble fluxes similar to DAF nozzles, but rather approximately one tenth the bubble flux. Nevertheless, the separation performance was on the same timescale as DAF cycles in the water sector. The inescapable conclusion is that, although there are at least an order of magnitude less collisions, the collision efficiency is highly effective. Turbulent shear might destroy nearly as many flocs as turbulence enhanced collision rate generates. Anecdotally, industrial experience in the water sector is that decreasing turbulence intensity generated by DAF nozzles, increases flotation separation rates (64). The DZ flotation approach, however, exceeds the bubble flux of conventional DAF nozzles in the target bubble size range, due to the nearly monodisperse population density and tuneability of FO (16).

3.4 Ion Flotation

Ion flotation involves the flotation from aqueous solution of non-surfactant ions, typically mediated by the formation of an insoluble surfactant complex with the oppositely charged surfactant. That complex should be tuned, typically by pH, to be hydrophobic and therefore attracted to the bubble phase. Microbubbles produced by the saturation nucleation method have shown to be sufficient for around 80% removal efficiency of cadmium

ions (65) or heavy metal ions (66). The biochemical aspect of this work is the identification of novel, green chemical biosurfactants that increase sustainability (66). Wan Nafi and Taseidifar (67) reviewed green chemical ion flotation, with a focus on biodegradable surfactants for toxic ion removal from aqueous solutions. In remediation uses for ion flotation, the contaminants are often at the parts per million level. The advantage of green chemical surfactants, which are often chemically transformed biosurfactants, is that they can be tailored for specific toxic ion recovery, while still maintaining biodegradability.

3.5 Solvent Sublation (Flotation)

Solvent sublation travels under many pseudonyms: liquid biphasic flotation and two-phase flotation are the other common terms for the process. An immiscible organic solvent layer is introduced on top of a bubble column aqueous phase. The approach aims to collect enriched material from the bubble surface, for which the solvent is selected for greater attractiveness than the aqueous solution for the material carried by the bubble. It is similar to liquid-liquid extraction, but with the distinction that liquid-liquid extraction is controlled by the equilibrium partitioning along the interface, whereas solvent sublation can have chemical thermodynamic drivers far from equilibrium.

The theory is well presented in Lemlich's book (58). The best review of the field is still the one written by Bi *et al.* (68). Since there is no need for mixing or waiting for phase equilibria, solvent sublation is a simple, low-cost technique. It needs only low solvent amounts relative to the aqueous layer, so scale-up is facile. Consequently, it has been successfully applied in the treatment of wastewater and enrichment stages for chromatographic analysis (68). Chew *et al.* (69) give an example of just how many degrees of freedom solvent sublation can tune for bespoke bioproduct recovery. In this instance, it is C-phycocyanin, a valued pigment, from a strain of *Spirulina*: "Various experimental parameters such as type of phase forming polymer and salt, concentration of phase forming components, system pH, volume ratio, air flotation time and crude extract concentration were evaluated to maximise the C-phycocyanin recovery yield and purity." Sankaran *et al.* (70) give a thorough review of the developments concerning biomacromolecule separations using solvent sublation.

Solvent sublation relies on selection of solvent in general, but a recent advance illustrates how bespoke the separation scheme design might need to be to achieve high removal efficiency and selectivity, particularly for product recovery. Zeng *et al.* (71) substituted a particle suspension for the aqueous solution beneath the organic solvent, introducing the degree of freedom of chromatographic-like adsorption-desorption dynamics to the particle suspension. The approach is, in this first instance, focused on the accumulation in the solvent layer, rather than elution. Zeng *et al.* report better separation and selectivity performance for particle suspension assisted solvent sublation to all other approaches for product recovery of two terpenoids from 'docking' with amyloid-β. As these terpenoids are bioproducts extracted from an aromatic herb plant, the implications for bioprocessing are clear. Customised separation schemes must be designed for effectiveness and high throughput.

The story is similar for Khoo *et al.* (72), who pioneered electropermeabilisation-assisted liquid biphasic flotation. This approach uses electroporation of cells in the aqueous phase to extract their content, with simultaneous bubble flux that carries metabolites to the organic top phase, resulting in this case in the selective removal of fucoxanthin, released from the diatom *Chaetoceros calcitrans*. There are many poration approaches and cell lysis methods that could replace electroporation for such as transformation, but electroporation also induces electric charge on microbubbles, so this approach might be better for tuning substrate specific flotation with microbubbles. However, electroporation also requires electrodes, which suffer from fouling by biomaterials and do not scale well to larger volumes of processing vessels.

De Araújo Padilha *et al.* (73) report yet another innovation as a variation on the theme of solvent sublation. Those authors added a second aqueous layer, *n*-octanol and PEG400/ammonium sulfate solution above the aqueous solution, for a three-phase flotation separation scheme aimed at vanillin recovery. The additional complexity aims to preferentially separate phenolic compounds from bioproduct mixtures, particularly for food additives.

The search on all of these pseudonyms for solvent sublation and microbubbles as keywords comes up nil in science citations using Web of Science™ abstracting service. The major microbubble parameter to varying is bubble size, which influences the rate of bubble absorption processes, but also, due to surface tension effects

with higher Gibbs free energy per unit area, influences the absorption-desorption process. Nevertheless, given the plethora of parameters that conventional solvent sublation can vary, let alone those introduced with recent innovations, there is substantial scope to improve downstream processing with bespoke microbubble mediated solvent sublation processes.

3.6 Hydrodynamics and Control of Flotation

All forms of flotation depend heavily on the hydrodynamics of three-phase motion, bubbles, liquid and particles. An excellent overview of hydrodynamics issues is given by Peleka and Matis (74). In general, the effects of forced convection *via* stirring, such as by impellers, control the contacting pattern of bubbles and substrates. The rate of collisions, floc formulation and floc breakup are largely controlled by hydrodynamics. Rulyov (75) reviewed the physicochemical hydrodynamic theory of flotation, exposing the key roles of surface electrodynamic and hydrodynamic forces in the aggregation of particles and bubbles to form flocs, as well as bubble coalescence, crucially dependent on size. In just about all flotation processes discussed in these generalised flotation processes, turbulence plays a central role as the dominant mechanism to create collisions. There are very few studies dealing with microhydrodynamics of generalised particles in laminar flow, with Grammatika and Zimmerman (76) describing the sea surface microlayer as a potential application area for such gentle interaction, dominated by the gas-liquid sea surface boundary condition or layer. Those authors idealised the initial microbubble field as uniformly sized and spaced, which had never at the time been even approximately achieved. Zimmerman *et al.* (7, 15) report on FO generated microbubble clouds that within the submerged plume are nearly monodisperse in size and spatially nearly uniformly distributed, so achieving low coalescence. Crucially, these microbubbles rise maintaining laminar flow.

There are only two ways accurately to quantify the hydrodynamics effects on flotation, experiment and modelling. For nanobubbles to microbubbles, experiments have recently been reviewed (77), with perhaps the most interesting approach being the use of two different bubble generation approaches to create conventional flotation bubble size distribution aimed at segregating the lions' share of the particles, and then micro- or nanobubbles generated by a separate device, simultaneously, aiming at collecting the fine particles (50). Three phase flotation processes require specialised diagnostic instrumentation to map particle dynamics as a route to exploring the hydrodynamic effects. Mesa *et al.* (78) demonstrate the benefits of positron emission particle tracking for exposing both particle dynamics and hydrodynamics, simultaneously.

The modelling of such multiphase flotation processes is problematic. In general, hybrid computational fluid dynamics and particle dynamics approaches are computationally intensive, even if statistical moments, such as Reynolds averaged turbulent flow fields with population balances for the bubble and particle distributions. Generally, much similar phenomenological models, for instance for foam drainage, that are semi-empirical in nature but can deal with geometrical variations, are practically useful (79). The entrainment factor is a particularly important phenomenological feature dependent on hydrodynamics (80), well correlated with flotation efficiency. The modelling of flotation, capturing hydrodynamic effects, that goes from the extremes of phenomenological to mechanistic approaches has been reviewed by Wang *et al.* (81). A related but very important issue is how hydrodynamics are central to the control of flotation processes, which has recently been reviewed (82).

What is clearly missing from the literature are equivalent efforts to characterise the hydrodynamics, either experimentally or by modelling, of microbubble mediated flotation separations of biological materials. The greater complexity of cell or microorganism interactions with microbubbles than simply solid particles with microbubbles requires considerable modification to modelling methods. A recent advance in modelling the hydrodynamics of different size and constituency of colloidal particles is the introduction of interaction chemical potentials to treat general diffusiophoretic motion, a more general class of motion that includes electrophoresis (83). For colloidal particles, the interaction chemical potential is repulsive at short separation distances between particles, which accounts for excluded volume effects. With more general particles including microbubbles, the interaction class potentials within particle classes and across classes have markedly different character. Such an approach would be complementary to the microhydrodynamics approach of Grammatika and Zimmerman (76) which did not treat chemical interaction potentials but hydrodynamics in Stokes flow only. Expanding

these interactions to cells or microorganisms as the particle would surely require some characterisation of individual particle-microbubble dynamics that is yet unexplored.

4. Self Assembled Microbubble and Microorganism Complexes

Among the first papers to proclaim absorptive bubble mediated separations for bioprocessing was by Fields *et al.* (52). The title of the paper placed the major effort of the work as bubble fractionation of bacteria, attaching to the bubbles, which implies separation is the achievement. But actually the major achievements were characterising the growth regimes of the *Pseudomonas methylotropha* on a methanol carbon source. The study was targeted to a bubble column because bacteria were known to be active on bubble interfaces (84), while designing the microbial system for a methanol-trophic microorganism on a methanol solution with embedded, dispersed bubbles was certain to attract methanol as a surfactant to the bubble interface. Simultaneous growth and bubble fractionation effects were observed.

Tropism is a powerful organising principle for microbial motion. In the work of Fields *et al.* (52), it was active preferentially for gradients of two nutrients, methanol and oxygen, which preferentially are present on the bubble interface. Microorganisms have long been known to swim up nutrient gradients, which can lead to macroscopic flow structures known as bioconvection (85, 86).

In this section, we provide evidence that microbubbles provide trophic attractors which can assemble into local ecologies. Gas exchange for co-cultures could be trophically attractive with more than one species of microorganism attached to the interface, in addition to the collection of microorganisms due to surfactant induced sticking factor for collisions being high for amphoteric microorganisms on microbubble interfaces. Gilmour and Zimmerman (1) labelled this phenomenon 'Desai artificial lichen', but it has also been termed 'Desai microbubble scaffolds' as the bubble size, gas composition, and surfactant additives can be designed, as demonstrated in Section 3, to achieve attractiveness of the microbubble scaffold selectively for a distinct occupancy of microorganisms. The purpose could be simultaneous or staged bioreaction engineering with product recovery, similar to Fields *et al.* (52) for bubble columns without dispersed microbubbles. Due to the collection efficiency of microbubble dispersions being tuneable, DAL/DMS can be designed to be effective for particular purposes.

This section is structured as follows. In Section 4.1, tropism as an attractor is discussed. In Section 4.2 the emerging fields of symbiotic and microbiome engineering provide a context for DAL/DMS as the microbubble bubble bank extension of such designed consortia. In Section 4.3, the meshing of the two prior subsections supports that DAL/DMS are components of a bioprocessing strategy to design and engineering optimal transforms of fermentation and separation, either distinctly or combined co-located or simultaneously, or both.

4.1 Tropism and Taxis Mechanisms for Aggregation of Microorganisms

Ouchi and Akiyama (87) show a microscope image depicting the affinity of a non-foaming yeast mutant towards an oxygen-rich coarse bubble. Yeasts are well-known to be oxygen starved, with conventional studies showing that DO levels in batch propagators typically crash to zero (8). Yeast cells are purportedly non-motile and are encased in a cell wall that supports high internal turgor pressure. Yet, unexpectedly morphogenetic changes led to reported motility of yeast during cell division (88). An explanation of the mechanism whereby cells decode complex spatiotemporal gradients is supported by recent studies in budding yeast cells of chemotactic motion of a polarity site (89). It is safe to conclude, however, that the non-foaming mutant motility seen in **Figure 11** from Ouchi and Akiyama's work (87) is atypical of wild type yeast, but illustrative that yeasts are attracted to nutrients by tropism and taxis, so that the reported microbubble adherence of yeasts and a mixed consortia of microalgae as DAL/DMS complexes in Section 3.1 and selectively floated (**Figure 6**) has a context in the literature. The collisions of microbubbles with yeast could be sufficiently sticky so that they maintain microbubble adherence. Palmieri *et al.* (90) found that yeasts were facile at flotation without foaming agents, and that dried yeast-rich foam collected from flotation had a high protein character, plausibly indicating that embedded cell wall proteins stabilise yeast attachment to bubbles. Raghavendran *et al.* (5) demonstrated that it expressed a substantially different protein profile of yeast propagated in a fermenter populated with dispersed microbubbles compared to the same media and strain at the same DO levels, but aerated by perfusion. The greatest difference in the profiles were for high

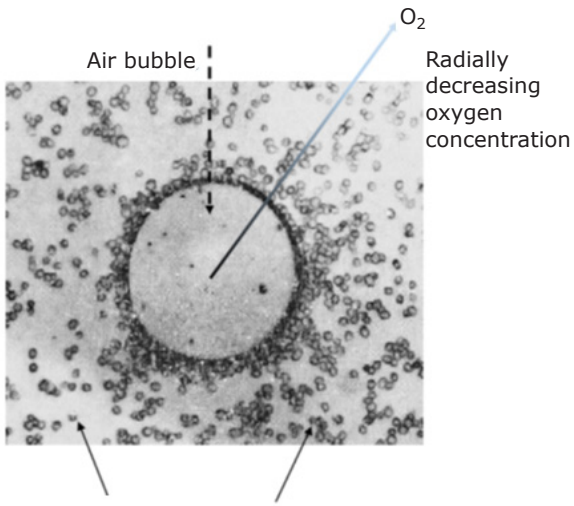

Fig. 11. Affinity of non-foaming mutant yeast to a coarse bubble (87). Wild-type yeast were removed from the culture by agglutination

levels of expression of proteins coding for cell wall metabolites, indicating that interaction between microbubbles and cell walls of yeast cells occurred frequently.

Microalgae have many strains that are known to exhibit chemotaxis, with particular physiology such as flagella that facilitate motility. Hu *et al.* (91) characterised motility levels for shear-damaged *Crypthecodinium cohnii* microalgal cells, which are dinoflagellate. The rate of motility was measured by image analysis using a trapped air bubble, shown in **Figure 12**. Clearly oxygen is a nutrient for this strain.

Ding *et al.* (92) showed visual evidence of microalgae (*Chlorella pyrenoidosa*) attaching to a growing CO_2 bubble injected through an orifice into a fermentation broth with a suspended microalgal bioculture, during before bubble detachment. In such circumstances, inert particles are displaced away from the gas-liquid interface of the bubble due to the liquid displacement current. In order to attach, the microalgae strain must overcome this inertial force, due either to electronic attractive forces or chemotaxis up the CO_2 gradient. The authors attribute the attachment to chemotaxis followed by capillary (surfactant) adherence. This attribution followed from surface tension reduction inferred from optical density measurements. Variations of CO_2 concentration were seen to influence the microalgal-bubble attachment frequency, through the proxy of bubble growth rate and final bubble diameter at attachment, which are related to surface tension hydrodynamically.

Pei *et al.* (93) found a very similar story occurs with a methanotrophic bacteria (*Methylosinus sporium*) suspended in a fermentation broth into which methane-rich bubbles were injected. The hydrodynamics of the bubble detachment, resultant bubble size and bubble rise times could be used to infer change in surface tension as well, due to observed bacterial chemotaxis and absorption. This scenario as a dual attraction to the bubble, which was a 50:50 (v/v) mixture of methane and oxygen, and *M. sporium* requires both nutrients for its metabolism. There is now a widespread gas fermentation community that studies production of useful bioproducts from either methane, hydrogen or carbon monoxide gases as feedstocks. The observed intensification of metabolic activity is consistent with the absorption of the bacteria on the bubble interface.

4.2 Synergistic Complexes of Microorganism Co-Cultures

Symbiotic engineering is a new term introduced to environmental remediation approaches that select

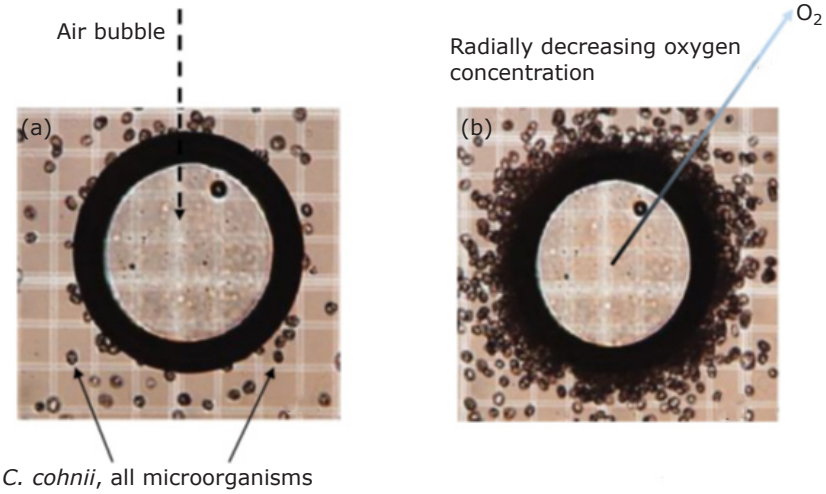

Fig. 12. Photographs of an air bubble trapped between a haemocytometer and the coverslip, the air bubble being surrounded by a suspension of motile *C. cohnii* microalgal cells: (a) all microorganisms, initially sparse density near the bubble interface; (b) radially decreasing oxygen concentration and chemotaxis of *C. cohnii* up the oxygen gradient after 1 min (91)

combinations of microorganisms from different strains to achieve different goals appropriate to the contamination (94). For instance, it is well known that bacteria produce CO_2 while requiring O_2, but microalgae require CO_2 and produce O_2. The appropriate strains could be produced to feed on a nutrient source in a wastewater that is potentially toxic to aquatic or human life to render it harmless. Or the floc is sedimented or floated for separation to densify the biomass and reduce the volume of toxic material. Indeed, a systematic approach for top down and bottom up (self-assembly) of microbiomes due to mutualism has recently been proposed (95) for metabolic function and self-organising spatial patterning.

Symbiotic engineering, however, uses the canonical liquid mediated dissolved gas and nutrient model. However, there have been many observations of clusters or attachments of microorganisms of different strains that achieve mutualism directly. Biofilms are such a class of symbiotic microorganisms but are anchored to surfaces. Dispersed mutual clusters in aqueous media are now commonly observed. For instance, Samo *et al.* (96) observed microalgal species (*Phaeodactylum tricornutum* and *Nannochloropsis salina*) using stable isotope tracing and high spatial resolution mass spectrometry imaging (NanoSIMS), characterising the effect of bacterial attachment. The widely varying carbon uptake rates for such clusters led to the conjecture that phycosphere-mediated, mutualistic chemical exchanges within autotrophs and heterotrophs complexes may be a fruitful means to increase microalgal productivity for applied engineering targets.

Similarly, Kazamia *et al.* (97) found a mutualism between a bacteria strain (*Mesorhizobium* sp.) and a microalgal strain *Chlamydomonas nivalis,* concerning the cobalamin metabolism for provision of vitamin B12. The later does not produce B12 independently, yet achieves a stable ratio of cells with *Mesorhizobium loti*, observed to produce cobalamin as a secreted metabolite, strongly suggesting the mutualism mechanism for cobalamin auxotrophy. Several tests were conducted to determine that mutualism persisted, although the biochemical support from microalgae *C. nivalis* provided to *M. loti* was not identified, the essential presence of the microalgae was determined. Immobilisation of the two species, however, determined that physical contact was not necessary for mutualism to occur, yet the dispersed microorganisms showed much greater metabolic function.

Ramanan *et al.* (98) review many such studies of microalgal-bacteria synergies in not just growth, but promotion of flocculation. The flocculation facilitation certainly means that direct contact between microalgae and the chosen bacteria strain is beneficial and promotes flocculation. Confocal laser scanning images merged with differential interference contrast microscopic images of several multicellular algae and their closest unicellular relative, where the bacteria were stained, show direct complexes occur where mutualism is observed in volvocine algae.

Fei *et al.* (99) explored the role of quorum sensing (QS) in stimulating, facilitating and regulating bacterial-microalgal interactions. Bacteria in the phycosphere use either chemotaxis or attachment to benefit from algal excretions. QS signalling biochemicals were systematically expressed or blocked in this study that coded for chemotaxis while stimulating attachment to demonstrate the essential role of attachment in forming algal symbionts that are inferred to populate the phycosphere. Stained species in micrographs with concomitant sequencing of the bacterial DNA demonstrated two diatom symbionts use autoinducers (acyl-homoserine lactones) molecules to inhibit their motility and enhance biofilm formation, processes that likely control their ability to attach to diatom transparent exopolymeric particles (TEP) and thus colonise the phycosphere. Forming biofilm on algal surfaces or algal TEP also protects bacteria against toxins and antibiotics and provides shelter from predation (100).

4.3 Desai Artificial Lichen as the Sum of Taxis and Tropism Bubble Microorganism Aggregation and Microorganism Symbiosis

In Section 4.1, examples of microorganism migration to bubble surfaces were given, with chemotaxis and absorption mechanisms accounting for the complexation. This is complementary to microbubble absorption mechanisms presented in Section 3. In section 4.2, the growing body of evidence of mutualism between specifically microalgae and bacteria were reviewed in the literature. These aspects of bubble complexed microorganisms and direct physical contact of heterogeneous microorganisms logically combine to the possibility of microbubbles complexing aggregates of more than one species of microorganism (DAL/DMS), with the benefits of

rapid gas exchange across the microbubble and rapid surfactant exchange along the microbubble interface, as described in Section 2.2.3 and illustrated by **Figure 1(d)**.

Microalgae-yeast DAL/DMS complexes were described in Section 3.1, expanding on the seminal description by Gilmour and Zimmerman (1). In particular, the capability to design the features of a DAL/DMS exploiting the combination of wettability and tropism or chemotaxis for selecting attraction to both microorganism species is an advance in the emerging field of symbiotic engineering. The flexibility for design extends not just to the self-assembly of the DAL/DMS, but also to designing subsequent separation schemes, largely based on flotation, but making *in situ* separation from the fermentation achievable. In general, *in situ* product removal has a beneficial effect on chemical reaction systems, by reducing the product activity, so favouring it by Le Chatelier's principle. The analogue role in bioreactor systems is played by reducing inhibition effects for biochemical, but also by decreasing competition for scarce resources, in the case of whole microorganism removal.

In Section 2.2.3, we closed with the mystery of how doubling methane production rates in AD with CO_2 microbubble sparging could be achieved with simply more interfacial area for mass transfer, given that methane is largely insoluble. The hypothesis that collisions or absorbance between microbubbles and methanogens was essential to explain such acceleration was posed, but with the caveat that collision-with-release probably have too little direct contacting time between the phases to explain the dramatic rate increase. The mystery is actually deeper.

Gilmour and Zimmerman (1) reported:

> "Direct microbubble contact with microorganisms 'short circuits' the need for slow dissolution of the nearly insoluble gases, and slow diffusion of dissolved gases through aqueous solution. Even higher levels of biogas production rate have been observed in industrial optimisation studies with much smaller average bubble sizes than in this lab bench proof-of-concept study, indicating the essential role of microbubble collision and coordination in direct microorganism-microbubble gas exchange."

With wet food waste AD and smaller microbubbles than the work by Al-Mashhadani *et al.* (26), bubble sizes were tuned using frequency and flowrate control so that the bubble bank of non-buoyant microbubbles is the dominant number density of the microbubble phase. These industrial trials with multiple replicants achieved repeatable observation that methane production reaches its limit after 2–4 days, with the same cumulative production as the control of unbubbled AD on the same feedstock which completes in 20–25 days.

Such an acceleration of production rate, an order of magnitude increase, seems improbable based on enhanced liquid mediated gas exchange alone, due to the seeding of the bubble bank with much greater surface area than conventional fine bubbles or even the ~550 μm average bubble size in Al-Mashhadani *et al.*'s work (26). If the *in situ* production removal of the inhibition effect of methane on methanogens is complete, then the next limitation must come from scarcity of nutrients. In a similar way to the slow removal of methane under conventional AD conditions, the delivery of hydrogen from the canonical liquid transport mechanisms reviewed in Section 2.1, must become the next most limiting step once methane removal is accelerated. Hydrogen is much less soluble in water than oxygen, by a factor of about 20, so methanogens are hydrogen starved. Thus methane production rate cannot exceed the hydrogen anabolism by methanogens, which is limited by hydrogen mass transfer flux.

Given that this much greater daily production rate of methane, greater than eight-fold increase, mediated by sub-100 μm diameter microbubbles seeded in the 5 min per day of sparging, hypotheses are needed for the mechanism. **Figure 13** provides one notion for the self-assembled DAL/DMS that can address the much more rapid provision of hydrogen from acetogens to methanogens than liquid-mediated mass transfer. Gas exchange occurs across the microbubble with soluble gases ammonia and CO_2 potentially equilibrating with the liquid boundary layer, but insoluble gases H_2 and methane provided a rapid route for gas exchange of waste gases of one species that are nutrients for another. Similarly, the interfacial transport of volatile fatty acids (VFA) between acidogens and acetogens is much more rapid than liquid mediation due to the surfactant attraction opposing diffusion through the liquid. The diffusion across the microbubble, even in the absence of internal bubble convection, if the interface of the microbubble is surfactant blocked, it occurs at least 10^4 times faster than liquid mediated mass transfer.

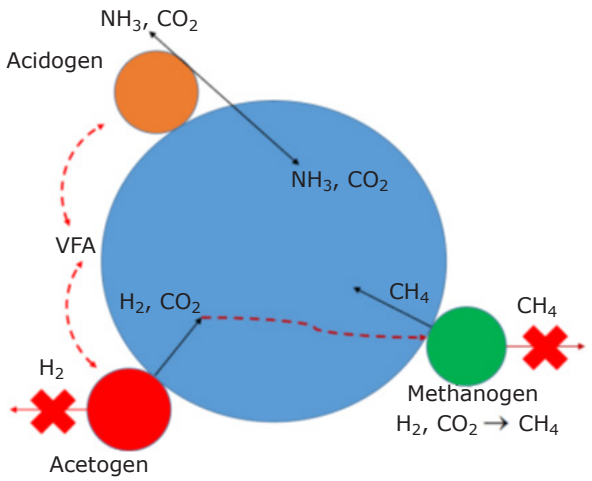

Fig. 13. Schematic of a self-assembled microbubble coordinated floc (DAL/DMS) of methanogens, acetogens and acidogens absorbed on the microbubble interface

Logically, the next limiting step is the provision of appropriate carbon-sources such as VFAs and other hydrolysis products to the acetogens and acidogens of the DAL/DMS through liquid mediation. As microbubbles grow according to their methane composition, they must rise, creating convection currents in the AD fermenter, improving the liquid missing, hence VFA and sugary material mass transfer in an otherwise unstirred vessel.

It should be noted that AD fits the requirements of an engineered microbiome (95). The hypothesis that DAL/DMS are the agents implementing the accelerated metabolism is wholly new. This paper provides arguments and evidence supporting this DAL/DMS approach that has been successful in engineering microbubble mediated microbiomes in yeast plus microalgae co-cultures, with DAL/DMS observed under the microscope before they were hypothesised, and in AD, inferred by the acceleration of methane production rates beyond known inhibition effects. It is well known that ammonia inhibits AD (101), so its removal by DAL/DMS would be facilitated if microbubbles also stripped ammonia. However, due to the dissolution and subsequent dissociation of ammonia in aqueous solution, special contacting patterns and conditions are required to recover substantial amounts of ammonia (6).

5. Summary and Conclusions

Naively, microbubbles should accelerate mass transfer in bioprocessing, fermentation and separation processes, due to the massive increase in interfacial area of the dispersed phase. Yes, surfactant-laden media, according to the classic textbook of Clift *et al.* (10), preferentially occupy the gas-liquid interface so provide substantial blockage to mass transfer. Nevertheless, the mass transfer coefficient two-film model of Bailey and Ollis (2) seems to fit experiments well, just introducing a correction factor (α) to account for the blockage, for either dosing or stripping experiments. However, the model would seemingly be inapplicable for nearly insoluble gases, for instance, hydrogen and methane in AD. Al-Mashhadani *et al.* (26, 27) showed that microbubbles seeded to just 5 min a day provide substantial enhancement of methane production rate that is unexplained by conventional two-film theory for dosing or stripping. Instead, it supports direct contact by either collision-and-release or collision-and-complex formation between the bubble bank of microbubbles and methanogens.

Subsequent decrease in the microbubble average size of the seeded disperse phase achieves greater than eight-fold increase in the production rate of biogas. This cannot be explained by dosing or stripping by either the classical two-film model of liquid-mediated gas exchange, nor even by collision and release, due to the obvious limitation of the supply of hydrogen gas to methanogens. Only the DAL/DMS hypothesis is consistent with the observation, with self-assembly of acetogens, acidogens and methanogens complexed by microbubbles. This provides a rapid gas exchange internally within a microbubble for microbes absorbed on the microbubble interface.

The DAL/DMS approach was first observed by the first author of the present work in experiments targeting the engineering of the microbiome of yeast and microalgae for synergy of metabolism, as well as potential for selective flotation separations. Absorptive (micro)bubble separation fermentation and separation bioprocessing has been observed and characterised over the past 50 years. The symbiotic engineering or microbiome engineering of microorganism consortia using heterotrophic microbes is a fairly recent phenomenon, aiming to achieve mutualism, typically for wastewater remediation bioprocessing. This article highlights the potential for engineering DAL/DMS for bioproduct production *via* fermentation, potentially linked with *in situ* product removal, or with flotation separations by design. These linked operations for

bioprocessing of products can be engineered by design with tuneable control.

Acknowledgments

The authors gratefully acknowledge the Engineering and Physical Sciences Research Council (EPSRC), UK, for supporting this work financially (Grant nos. EP/N011511/1, EP/P030238/1, EP/K001329/1, EP/I019790/1). InnovateUK, IIKE, The Royal Society, AECOM Design Build, and Viridor are acknowledged for funding support. The many colleagues who have contributed discussions and technical support leading to the insights in this paper, including: M. Al-Mashhadani, H. Bandulasena, V. Tesař, H. Mohammed, S. R. Taylor, C. Hardacre, J. Jacquemin, S. Brittle, L. Tse, W. Zhou, P. Verrier, E. Baril, W. Nugroho, Y. Sharma, G. Yadav, U. Haji Hassan, M. du Prees Thomas, E. Akototse, H. Khudair, B. Franklin, G. Medley, M. Hines, J. Pandhal, H. Jensen, D. J. Gilmour and S. Vaidyanathan, are thanked for their assistance.

Glossary

a	Specific area = total bubble interfacial area divided by total phase volume, m^{-1}
α	Effectiveness fraction for mass transfer phenomenologically observed (ratio)
c, c_0	Optical density; at the initial time, reported as unitless ratio
c_l	Concentration (or titre) of a dissolved gas, molarity or mg l^{-1}
c_l^*	Concentration (or titre) of a dissolved gas at saturation, molarity or mg l^{-1}
$c_{l,\,crit}$	Critical liquid dissolved gas concentration demarking degassing from dosing
γ	Surface tension, N m^{-1}
γ_i	Activity coefficient in liquid phase (unitless)
H	Henry's Law Coefficient (ratio, no units)
ΔH_{vap}	Enthalpy change of vaporisation at boiling point, kJ mol^{-1}
J	Specific molar flux of dissolved gas, mol m^{-3} s^{-1}
j_i	Interfacial molar flux of gas for process i, mol m^{-2} s^{-1}
k_i	Mass transfer coefficient of species i, m s^{-1}
K_l	Liquid boundary layer side mass transfer coefficient, m s^{-1}
K_g	Gas boundary layer side mass transfer coefficient, m s^{-1}
K_L	Overall mass transfer coefficient for two film theory, m s^{-1}
K	Partition coefficient, ratio of concentration on the bubble interface to the concentration in the bulk, m^{-1}
MEA	Monoethanolamine
$\dot{n}_i$	Molar flux of species i
P_i*	Saturation pressure at the temperature in the microbubble phase of species i, bar
P_i	Partial pressure at the temperature in the microbubble phase of species i, bar
R	Specific oxygen uptake rate per unit mass of fermenting microorganisms, s^{-1} l^{-1} or s^{-1} m^{-3}
R	Gas constant, J mol^{-1} K^{-1}
T	Absolute temperature, K
T_b	Boiling point of species i, K
V	Volume of phase
vvm	Volume of air sparged (in aerobic cultures) per unit volume of growth medium per minute, typically used in fermentation
x_i	Mole fraction of species i in the liquid phase

References

1. D. J. Gilmour, W. B. Zimmerman, 'Microbubble Intensification of Bioprocessing', in "Advances in Microbial Physiology", ed. R. K. Poole, Ch. 1, Vol. 77, Elsevier Ltd, London, UK, 2020, pp. 1–35
2. J. E. Bailey, D. F. Ollis, "Biochemical Engineering Fundamentals", 2nd Edn., McGraw Hill, New York, USA, 1986
3. M. K. H. Al-Mashhadani, S. J. Wilkinson, W. B. Zimmerman, *Chem. Eng. Sci.*, 2015, **137**, 243
4. W. Fan, P. Desai, W. B. Zimmerman, Y. Duan, J. C. Crittenden, C. Wang, M. Huo, *J. Clean. Prod.*, 2021, **294**, 126258
5. V. Raghavendran, J. P. Webb, M. L. Cartron, V. Springthorpe, T. R. Larson, M. Hines, H. Mohammed, W. B. Zimmerman, R. K. Poole, J. Green, *Biotechnol. Biofuels*, 2020, **13**, 104
6. P. D. Desai, M. Turley, R. Robinson, W. B. Zimmerman, *Chem. Eng. Process.: Process Intensif.*, 2022, **180**, 108693
7. W. B. Zimmerman, M. Zandi, H. C. H. Bandulasena, V. Tesař, D. J. Gilmour, K. Ying, *Appl. Energy*,

2011, **88**, (10), 3357

8. J. Hanotu, D. Kong, W. B. Zimmerman, *Food Bioprod. Process.*, 2016, **100**, (A), 424
9. N. Harnby, M. F. Edwards, A. W. Nienow, "Mixing in the Process Industries", 2nd Edn., Butterworth-Heinemann, Oxford, UK, 1992
10. R. Clift, J. R. Grace, M. E. Weber, "Bubbles, Drops, and Particles", Academic Press Inc, New York, USA, 1978
11. G. Schulze, E. U. Schlünder, *Chem. Eng. Process.: Process Intensif.*, 1985, **19**, (5), 257
12. D. Rosso, M. K. Stenstrom, *Water Res.*, 2006, **40**, (7), 1397
13. A. W. Nienow, *Cytotechnology*, 2006, **50**, (1–3), 9
14. J. Hanotu, H. C. H. Bandulasena, W. B. Zimmerman, *Biotechnol. Bioeng.*, 2012, **109**, (7), 1663
15. W. B. Zimmerman, V. Tesař, H. C. H. Bandulasena, *Curr. Opin. Colloid Interface Sci.*, 2011, **16**, (4), 350
16. P. D. Desai, M. Hines, Y. Riaz, W. Zimmerman, *Energies*, 2018, **11**, (10), 2680
17. F. Rehman, G. J. D. Medley, H. Bandulasena, W. B. J. Zimmerman, *Environ. Res.*, 2015, **137**, 32
18. B. Bandyopadhyay, A. E. Humphrey, H. Taguchi, *Biotechnol. Bioeng.*, 2009, **104**, (5), 841
19. K. Ying, D. J. Gilmour, W. B. Zimmerman, *Int. J. Mol. Sci.*, 2015, **16**, (5), 11509
20. Th. de Donder, "L'Affinité", ed. P. Van Rysselberghe, Gauthier-Villars, Paris, France, 1936
21. I. Prigogine, "From Being to Becoming: Time and Complexity in the Physical Sciences", W. H. Freeman and Company, San Francisco, USA, 1980
22. N. N. Abdulrazzaq, B. H. Al-Sabbagh, J. M. Rees, W. B. Zimmerman, *Ind. Eng. Chem. Res.*, 2016, **55**, (50), 12909
23. V. Tesař, C.-H. Hung, W. B. Zimmerman, *Sensors Actuators A: Phys.*, 2006, **125**, (2), 159
24. G. W. C. Kaye, T. H. Laby, "Tables of Physical and Chemical Constants and Some Mathematical Functions", 15th Edn., Longman, New York, USA, 1986, p. 219
25. R. M. Worden, M. D. Bredwell, A. J. Grethlein, 'Engineering Issues in Synthesis-Gas Fermentations', ACS Symposium Series, Vol. 666, Ch. 18, American Chemical Society, Washington, DC, USA, 1997, pp. 320–335
26. M. K. H. Al-Mashhadani, S. J. Wilkinson, W. B. Zimmerman, *Chem. Eng. Sci.*, 2016, **156**, 24
27. M. K. H. Al-Mashhadani, 'Application of Microbubbles Generated by Fluidic Oscillation in the Anaerobic Digestion Process', PhD Thesis, Chemical and Biological Engineering Department, University of Sheffield, UK, February, 2013, 276 pp
28. M. K. H. Al-Mashhadani, H. C. H. Bandulasena, W. B. Zimmerman, *Ind. Eng. Chem. Res.*, 2012, **51**, (4), 1864
29. P. D. Desai, W. C. Ng, M. J. Hines, Y. Riaz, V. Tesar, W. B. Zimmerman, *Colloids Interfaces*, 2019, **3**, (4), 65
30. D. Chatterjee, P. Jain, K. Sarkar, *Phys. Fluids*, 2005, **17**, (10), 100603
31. W. B. Zimmerman, M. K. H. Al-Mashhadani, H. C. H. Bandulasena, *Chem. Eng. Sci.*, 2013, **101**, 865
32. V. Tesař, *Chem. Eng. J.*, 2014, **235**, 368
33. M. Krzan, J. Zawala, K. Malysa, *Colloids Surf. A: Physicochem. Eng. Asp.*, 2007, **298**, (1–2), 42
34. G. Dhanarajan, P. Patra, V. Rangarajan, P. Somasundaran, R. Sen, *ACS Sustain. Chem. Eng.*, 2018, **6**, (3), 4046
35. S. Singhal, C. C. Moser, M. A. Wheatley, *Langmuir*, 1993, **9**, (9), 2426
36. M. Takahashi, *J. Phys. Chem. B*, 2005, **109**, (46), 21858
37. Q. Xu, M. Nakajima, S. Ichikawa, N. Nakamura, P. Roy, H. Okadome, T. Shiina, *J. Colloid Interface Sci.*, 2009, **332**, (1), 208
38. J. K. Edzwald, *Water Res.*, 2010, **44**, (7), 2077
39. Z. Dai, D. Fornasiero, J. Ralston, *Adv. Colloid Interface Sci.*, 2000, **85**, (2–3), 231
40. J. A. Kitchener, R. J. Gochin, *Water Res.*, 1981, **15**, (5), 585
41. M. R. Teixeira, M. J. Rosa, *Sep. Purif. Technol.*, 2006, **52**, (1), 84
42. M. R. Teixeira, V. Sousa, M. J. Rosa, *Water Res.*, 2010, **44**, (11), 3337
43. J. Hanotu, H. C. H. Bandulasena, T. Y. Chiu, W. B. Zimmerman, *Int. J. Multiph. Flow*, 2013, **56**, 119
44. J. Hanotu, E. Karunakaran, H. Bandulasena, C. Biggs, W. B. Zimmerman, *Biochem. Eng. J.*, 2014, **82**, 174
45. D. W. Fuerstenau, Pradip, *Adv. Colloid Interface Sci.*, 2005, **114–115**, 9
46. R. P. Feynman, *Eng. Sci.*, 1960, **23**, (5), 22
47. D. Weaire, S. Hutzler "The Physics of Foams", Oxford University Press Inc, New York, USA, 1999
48. R. Farajzadeh, S. Vincent-Bonnieu, N. Bourada Bourada, *J. Soft Matter*, 2014, 145352
49. A. Yehia, M. I. Al-Wakeel, *Miner. Eng.*, 2000,

13, (1), 111

50. J. Wang, L. Wang, J. Hanotu, W. B. Zimmerman, *Fuel Process. Technol.*, 2017, **165**, 131
51. R. Lemlich, *AIChE J.*, 1966, **12**, (4), 802
52. P. R. Fields, P. J. Fryer, N. K. H. Slater, G. P. Woods, *Chem. Eng. J.*, 1983, **27**, (1), B3
53. A. Suzuki, H. Maruyama, H. Seki, *J. Chem. Eng. Japan*, 1996, **29**, (5), 794
54. S. F. R. Taylor, S. A. Brittle, P. Desai, J. Jacquemin, C. Hardacre, W. A. Zimmerman, *Phys. Chem. Chem. Phys.*, 2017, **19**, (22), 14306
55. K. Sanderson, *Nature*, 2012
56. P. Desai, S. Jaffe, W. Zimmerman, 'Leidenfrost Like Effect Exhibited by Microbubbles for Biological Systems such as Anaerobic Fermenters', Biotech France 2017 International Conference and Exhibition, Paris, France, 28th–30th June, 2017, Setcor Media FZ-LLC, Dubai, UAE, 2017
57. A. Al-yaqoobi, D. Hogg, W. B. Zimmerman, *Int. J. Chem. Eng.*, 2016, 5210865
58. "Adsorptive Bubble Separation Techniques", ed. R. Lemlich, Academic Press Inc, New York, USA, 1972
59. A. N. Clarke, D. J. Wilson, "Foam Flotation: Theory and Applications", Marcel Dekker, New York, USA, 1983
60. L. Alexandrova, L. Grigorov, *Int. J. Miner. Process.*, 1996, **48**, (1–2), 111
61. M. Santander, L. Valderrama, M. Guevara, J. Rubio, *Miner. Eng.*, 2011, **24**, (9), 1010
62. G. Pooja, P. S. Kumar, S. Indraganti, *Chemosphere*, 2022, **287**, (2), 132231
63. K. E. Waters, K. Hadler, J. J. Cilliers, *Miner. Eng.*, 2008, **21**, (12–14), 918
64. B. Franklin, AECOM Design Build, UK, private communication, 2015
65. A. I. Alwared, N. Abdulrazzaq, B. Al-Sabbagh, *Iraqi J. Chem. Pet. Eng.*, 2019, **20**, (2), 1
66. X. Z. Yuan, Y. T. Meng, G. M. Zeng, Y. Y. Fang, J. G. Shi, *Colloids Surfaces A: Physicochem. Eng. Asp.*, 2008, **317**, (1–3), 256
67. A. W. Nafi, M. Taseidifar, *J. Environ. Manage.*, 2022, **319**, 115666
68. P. Bi, H. Dong, J. Dong, *J. Chromatogr. A*, 2010, **1217**, (16), 2716
69. K. W. Chew, S. R. Chia, R. Krishnamoorthy, Y. Tao, D.-T. Chu, P. L. Show, *Bioresour. Technol.*, 2019, **288**, 121519
70. R. Sankaran, R. A. P. Cruz, P. L. Show, C. Y. Haw, S. H. Lai, E.-P. Ng, T. C. Ling, *Fluid Phase Equilib.*, 2019, **501**, 112271
71. J. Zeng, W. Wang, J. Lin, Y. Zhang, H. Li, J. Liu, C. Yan, Y. Gu, Y. Wei, *J. Chromatogr. A*, 2022, **1674**, 463125
72. K. S. Khoo, C. W. Ooi, K. W. Chew, S. R. Chia, S. C. Foo, H. S. Ng, P. L. Show, *J. Chromatogr. A*, 2022, **1668**, 462915
73. C. E. de A. Padilha, C. da C. Nogueira, H. N. Almeida, W. R. D. B. de Medeiros, M. A. Oliveira Filho, J. S. de Araújo, E. S. dos Santos, *Food Bioprod. Process.*, 2020, **120**, 151
74. E. N. Peleka, K. A. Matis, *Open Chem.*, 2016, **14**, (1), 132
75. N. Rulyov, 'Colloidal-Hydrodynamic Theory of Flotation', Science Direct Working Paper No. S1574-0331(04)70477-4, SSRN–Elsevier, New York, USA, March, 2001, 22 pp
76. M. Grammatika, W. B. Zimmerman, *Dyn. Atmos. Ocean.*, 2001, **34**, (2–4), 327
77. G. Z. Kyzas, A. C. Mitropoulos, *Nanomaterials*, 2021, **11**, (10), 2592
78. D. Mesa, M. van Heerden, K. Cole, S. J. Neethling, P. R. Brito-Parada, *Chem. Eng. Sci.*, 2022, **260**, 117842
79. P. Grassia, S. J. Neethling, J. J. Cilliers, *Eur. Phys. J. E*, 2002, **8**, (S1), 517
80. S. J. Neethling, J. J. Cilliers, *Int. J. Miner. Process.*, 2009, **93**, (2), 141
81. G. Wang, L. Ge, S. Mitra, G. M. Evans, J. B. Joshi, S. Chen, *Miner. Eng.*, 2018, **127**, 153
82. P. Quintanilla, S. J. Neethling, P. R. Brito-Parada, *Miner. Eng.*, 2021, **162**, 106718
83. C. R. Rees-Zimmerman, A. F. Routh, *J. Fluid Mech.*, 2021, **928**, A15
84. A. Thomas, M. A. Winkler, "Topics in Enzyme and Fermentation Biotechnology", ed. A. Wiseman, Ellis Horwood, Chichester, UK, 1977
85. T. J. Pedley, N. A. Hill, J. O. Kessler, *J. Fluid Mech.*, 1988, **195**, 223
86. N. A. Hill, T. J. Pedley, *Fluid Dynam. Res.*, 2005, 37, (1–2), 1
87. K. Ouchi, H. Akiyama, *Agric. Biol. Chem.*, 1971, **35**, (7), 1024
88. I. Flor-Parra, M. Bernal, J. Zhurinsky, R. R. Daga, *Biol. Open*, 2014, **3**, (1), 108
89. D. Ghose, K. Jacobs, S. Ramirez, T. Elston, D. Lew, *Proc. Natl. Acad. Sci.*, 2021, **118**, (22), e2025445118
90. M. C. Palmieri, W. Greenhalf, C. Laluce, *Biotechnol. Bioeng.*, 1996, **50**, (3), 248
91. W. Hu, R. Gladue, J. Hansen, C. Wojnar, J. J. Chalmers, *Biotechnol. Prog.*, 2010, **26**, (1), 79
92. Y.-D. Ding, S. Zhao, X. Zhu, Q. Liao, Q. Fu, Y. Huang, *Clean Technol. Environ. Policy*, 2016, **18**, (7), 2039
93. H.-S. Pei, C.-L. Guo, G.-F. Zhang, Q.-Y. Tang, F.-Q. Guo, *Int. J. Heat Mass Transf.*, 2017, **110**, 873

94. A. I. Hossain, B. S. Baghirzade, O. Apul, M. J. Kirisits, S. Dev, S. Das, S. Islam, C.-Y. Lai, H. P. Huntington, S. Umanzor, W.-T. Chen, S. Aggarwal, N. B. Saleh, *ACS EST Engg.*, 2022, **2**, (4), 606
95. C. E. Lawson, W. R. Harcombe, R. Hatzenpichler, S. R. Lindemann, F. E. Löffler, M. A. O'Malley, H. García Martín, B. F. Pfleger, L. Raskin, O. S. Venturelli, D. G. Weissbrodt, D. R. Noguera, K. D. McMahon, *Nat. Rev. Microbiol.*, 2019, **17**, (12), 725
96. T. J. Samo, J. A. Kimbrel, D. J. Nilson, J. Pett-Ridge, P. K. Weber, X. Mayali, *Environ. Microbiol.*, 2018, **20**, (12), 4385
97. E. Kazamia, H. Czesnick, T. T. Van Nguyen, M. T. Croft, E. Sherwood, S. Sasso, S. J. Hodson, M. J. Warren, A. G. Smith, *Environ. Microbiol.*, 2012, **14**, (6), 1466
98. R. Ramanan, B.-H. Kim, D.-H. Cho, H.-M. Oh, H.-S. Kim, *Biotechnol. Adv.*, 2016, **34**, (1), 14
99. C. Fei, M. A. Ochsenkühn, A. A. Shibl, A. Isaac, C. Wang, S. A. Amin, *Environ. Microbiol.*, 2020, **22**, (11), 4761
100. C. C. C. R. de Carvalho, *Front. Mar. Sci.*, 2018, **5**, 126
101. Z. Zheng, Y. Cai, Y. Zhang, Y. Zhao, Y. Gao, Z. Cui, Y. Hu, X. Wang, *Water Res.*, 2021, **188**, 116466

The Authors

Pratik Desai is a global award-winning chemical engineer. He has developed, co-invented or invented several disruptive technologies including microbubbles, micro/nanodroplets and near-isothermal phase separations. He has been a techno-management consultant and advises several large corporations in multiple sectors delivering millions of pounds in savings. He has advised governmental organisations and Fortune 500 corporations and is considered a global subject matter expert by these for mass transfer, fermentation, and phase separations. He has global business interests, is an early-stage investor and sits on the board of several organisations. He sits on the UKRI Algae-UK management board.

Professor Will Zimmerman, a graduate of Princeton and Stanford Universities in the USA, has been recognised with five research fellowships from the National Science Foundation, NATO, the EPSRC, the Royal Academy of Engineering and the Leverhulme Trust. He was the sole winner of the Royal Society Innovation Award (Brian Mercer Fund) in 2010 for his invention and subsequent applications of fluidic oscillation generated microbubbles. He has authored over 200 academic publications including two bestselling textbooks, while co/creative inventor of seven patent families.